Mittuniversitetet
MID SWEDEN UNIVERSITY

Thesis for the degree of Doctor of Technology, Sundsvall 2008

WOOD AND FIBRE MECHANICS RELATED TO THE THERMOMECHANICAL PULPING PROCESS

Jan-Erik Berg

Supervisors:
Per Engstrand
Per A. Gradin

FSCN - Fibre Science and Communication Network
Department of Natural Sciences, Engineering and Mathematics
Mid Sweden University, SE-851 70 Sundsvall, Sweden

ISSN 1652-893X,
Mid Sweden University Doctoral Thesis 63
ISBN 978-91-86073-15-2

FSCN

Fibre Science and Communication Network
- ett skogsindustriellt forskningsprogram vid Mittuniversitetet

Akademisk avhandling som med tillstånd av Mittuniversitetet i Sundsvall framläggs till offentlig granskning för avläggande av teknologie doktorsexamen fredag, 21 november, 2008, klockan 10.00 i sal O 102 (SCA-salen), Mittuniversitetet Sundsvall.
Seminariet kommer att hållas på svenska.

WOOD AND FIBRE MECHANICS RELATED TO THE THERMOMECHANICAL PULPING PROCESS

Jan-Erik Berg

FSCN - Fibre Science and Communication Network
Department of Natural Sciences, Engineering and Mathematics
Mid Sweden University, SE-851 70 Sundsvall
Sweden

Telephone: +46 (0)771-975 000

Printed by Kopieringen Mittuniversitetet, Sundsvall, Sweden, 2008

WOOD AND FIBRE MECHANICS RELATED TO THE THERMOMECHANICAL PULPING PROCESS

Jan-Erik Berg

FSCN - Fibre Science and Communication Network
Department of Natural Sciences, Engineering and Mathematics
Mid Sweden University, SE-851 70 Sundsvall, Sweden
ISSN 1652-893X, Mid Sweden University Doctoral Thesis 63
ISBN 978-91-86073-15-2

ABSTRACT

The main objective of this thesis was to improve the understanding of some aspects on wood and fibre mechanics related to conditions in the thermomechanical pulping process. Another objective was to measure the power distribution between the rotating plates in a refiner.

The thesis comprises the following parts:

- A literature review aimed at describing fracture in wood and fibres as related to the thermomechanical pulping process
- An experimental study of fracture in wood under compression, at conditions similar to those in feeding of chips into preheaters and chip refiners
- An experimental study of the effect of impact velocity on the fracture of wood, related to conditions of fibre separation in the breaker bar zone in a chip refiner
- A micromechanical model of the deterioration of wood fibres, related to the development of fibre properties during the intense treatment in the small gap in the refining zone
- Measurements of the power distribution in a refiner.

The fracture in wood under compression was investigated by use of acoustic emission monitoring. The wood was compressed in both lateral and longitudinal directions to predict preferred modes of deformation in order to achieve desired irreversible changes in the wood structure. It was concluded that the most efficient compression direction in this respect is longitudinal. Preferable temperature at which the compression should be carried out and specific energy input needed in order to achieve substantial changes in the wood structure were also given.

The fibre separation step and specifically the effect of impact velocity on the fracture energy were studied by use of a falling weight impact tester. The fracture surfaces were also examined under a microscope. An increase in impact velocity resulted in an increase in fracture energy.

In the thermomechanical pulping process the fibres are subjected to lateral compression, tension and shear which causes the creation of microcracks in the fibre wall. This damage reduces the fibre wall stiffness. A simplified analytical model is presented for the prediction of the stiffness degradation due to the damage state in a wood fibre, loaded in uni-axial tension or shear. The model was based on an assumed displacement field together with the minimum total potential energy theorem. For the damage development an energy criterion was employed. The model was applied to calculate the relevant stiffness coefficients as a function of the damage state. The energy consumption in order to achieve a certain damage state in a softwood fibre by uniaxial tension or shear load was also calculated. The energy consumption was found to be dependent on the microfibril angle in the middle secondary wall, the loading case, the thicknesses of the fibre cell wall layers, and conditions such as moisture content and temperature. At conditions, prevailing at the entrance of the gap between the plates in a refiner and at relative high damage states, more energy was needed to create cracks at higher microfibril angles. The energy consumption was lower for earlywood compared to latewood fibres. For low microfibril angles, the energy consumption was lower for loading in shear compared to tension for both earlywood and latewood fibres. Material parameters, such as initial damage state and specific fracture energy, were determined by fitting of input parameters to experimental data.

Only a part of the electrical energy demand in the thermomechanical pulping process is considered to be effective in fibre separation and developing fibre properties. Therefore it is important to improve the understanding of how this energy is distributed along the refining zone.

Investigations have been carried out in a laboratory single-disc refiner. It was found that a new developed force sensor is an effective way of measuring the power distribution within the refining zone. The collected data show that the tangential force per area and consequently also the power per unit area increased with radial position.

The results in this thesis improve the understanding of the influence of some process parameters in thermomechanical pulping related wood and fibre mechanics such as loading rate, loading direction, moisture content and temperature to separate the fibres from the wood and to achieve desired irreversible changes in the fibre structure. Further, the thesis gives an insight of the spatial energy distribution in a refiner during thermomechanical pulping.

Keywords: Acoustic emission, Chips, Compression tests, Defibration, Disc refiners, Energy consumption, Fibre structure, Force sensors, Fracture, Impact strength, Mathematical analysis, Moisture content, *Picea abies*, Refining, Stiffness degradation, Strains, Temperature, Thermomechanical pulping, Velocity

SAMMANFATTNING

Det huvudsakliga syftet med föreliggande avhandling var att öka förståelsen för några aspekter av ved- och fibermekanik i samband med betingelser som råder vid framställning av mekanisk massa. Ytterligare ett syfte var att mäta den radiella effektfördelningen mellan de roterande skivorna i en raffinör.

Avhandlingen består av följande delar:

- En litteratursammanfattning över brott i ved och fibrer i samband med framställning av mekanisk massa
- En experimentell undersökning av brott i veden vid kompression vid betingelser som råder vid inmatning av flis till förvärmare och raffinörer
- En experimentell undersökning av slaghastighetens inverkan på brott i veden vid betingelser som råder vid defibrering i den inledande grovmönstrade malzonen
- En mikromekanisk modell av vedfiberns nedbrytning i samband med att fiberegenskaper utvecklas i den intensiva bearbetningen i den smala spalten mellan skivorna i den avslutande raffineringszonen
- Mätning av den radiella effektfördelningen mellan de roterande skivorna i en raffinör.

Brott i ved under kompression undersöktes med hjälp av akustisk emmisionsteknik. Veden komprimerades både lateralt och longitudinellt för att förutsäga vilka belastningsfall som är att föredra för att ge vedstrukturen irreversibla förändringar. Slutsatsen var att longitudinell kompression var den mest effektiva i denna bemärkelse. Vidare angavs vid vilken temperatur kompressionen bör utföras samt den specifika energiförbrukning som behövs för att uppnå betydande förändringar i vedstrukturen.

Fiberseparationsfasen och speciellt brottenergins beroende av slaghastigheten studerades med hjälp av en fallhammare och brottytorna studerades i mikroskop. Slutsatsen var att ökad slaghastighet resulterade i ökad brottenergi.

Vid framställning av mekanisk massa utsätts fibrerna för kompression tvärs fiberriktningen, drag och skjuvning vilket leder till mikrosprickor i fiberväggen och därigenom reduceras fiberväggens styvhet.

En förenklad analytisk modell presenteras som förutsäger styvhetsreduktionen pga. skadetillståndet i en vedfiber som belastas enaxligt i drag eller skjuvning.

Modellen baserades på en lämplig förskjutningsansats tillsammans med satsen om potentiella energins minimum. Ett energikriterium användes för att beräkna skadans utveckling. Genom att tillämpa modellen på ett specifikt exempel kunde relevanta styvhetskoefficienter beräknas som funktion av skadetillståndet.

Energiförbrukningen för att uppnå ett visst skadetillstånd visade sig vara beroende av mikrofibrillvinkeln i den mellersta sekundärväggen, belastningsfall, tjocklekarna på fiberväggens skikt och betingelser som fukthalt och temperatur. Vid betingelser liknade de som råder vid ingången av spalten mellan skivorna i en raffinör var energiförbrukningen mestadels lägre för vårvedsfibrer i jämförelse med sommarvedsfibrer. Materialparametrar som initialt skadetillstånd och specifik brottenergi bestämdes genom anpassning av indata till experimentella data.

Endast en del av elenergibehovet vid termomekanisk massaframställning betraktas som effektiv för fiberseparation och utvecklande av fiberegenskaper. Det är därför viktigt att öka förståelsen hur denna energi fördelas längs raffineringszonen.

Försök har utförts i en skivraffinör i laboratorieskala. En nyutvecklad kraftgivare visade sig vara effektiv vid mätning av energifördelningen i raffineringszonen. Insamlade data visade att den tangentiella kraften per ytenhet och därigenom även effekten per ytenhet ökar med radiell position.

Resultaten i denna avhandling ökar förståelsen för inverkan av några processparametrars betydelse för ved- och fibermekanik vid termomekanisk massaframställning som belastningshastighet, belastningsriktning, fukthalt och temperatur för att separera veden till fibrer och att uppnå önskade irreversibla förändringar i fiberstrukturen. Vidare ger avhandlingen en insikt i hur energin fördelas i en raffinör vid termomekanisk massaframställning.

TABLE OF CONTENTS

LIST OF PAPERS

This thesis is mainly based on the following five papers, herein referred to by their Roman numerals:

Paper I **Effect of Temperature on Fracture of Spruce in Compression, Investigated by Use of Acoustic Emission Monitoring**
J.-E. Berg and P.A. Gradin
J. Pulp Paper Sci. Vol 26 No. 8, August 2000, pp 294-299

Paper II **Effect of impact velocity on the fracture of wood as related to the mechanical pulping process**
J.-E. Berg
Wood Sci. Tech. Vol 35 No.4, August 2001, pp 343-351

Paper III **A Micromechanical Model of the Deterioration of a Wood Fibre**
J.-E. Berg and P.A. Gradin
J. Pulp Paper Sci. Vol 25 No. 2, February 1999, pp 66-71

Paper IV **On the energy consumption for crack development in fibre wall in disc refining - A micromechanical approach**
J.-E. Berg, M.E. Gulliksson and P.A. Gradin
Accepted for publication in *Holzforschung*

Paper V **Measurement of the Power Distribution in a Single Disc Refiner**
P. A. Gradin, O. Johansson, J.-E. Berg and S. Nyström
J. Pulp Paper Sci. Vol 25 No. 11, November 1999, pp 384-387

1 INTRODUCTION

Fibres are the main component in all paper grades and the by far most common source of fibres is wooden materials. In pulping processes fibres are separated from wood by chemical and/or mechanical means.

In chemical pulping processes most of the wood lignin and some of the hemicelluloses are dissolved and the individual fibres are made flexible by beating at relatively low energy input. Chemical pulps are suitable in products with demands on high strength e.g. liner board or brightness stability e.g. fine papers.

In mechanical pulping processes, on the other hand, only a few percentages of the wood components are dissolved. The wood structure is separated into a mix of individual fibres with intact length from the native wood, broken fibres and material peeled off from the outer part of the fibre wall, so called fines. The amount of electrical energy needed is considerable to make the fibre material flexible. Mechanical pulps are suitable for thin products with demands on high opacity e.g. newsprint and magazine papers or in products with demands on high bulk and stiffness as e.g. paperboards.

In mechanical pulping processes wood is mechanically transferred into pulp by repeated mechanical action either by pulpstone grits in wood grinding or by refiner bars in chip refining. In the following wood grinding will be excluded when using the term "mechanical pulping".

Mechanical pulping involves unit processes as chipping, chip washing, presteaming, refining, screening and bleaching. Refiner mechanical pulps (RMP) are produced without any presteaming of the chips and in atmospheric refiners. Thermomechanical pulps (TMP) are produced in steam pressurized refiners after preheating during a few seconds up to a couple of minutes at 115 to 155°C and chemithermomechanical pulps (CTMP) are produced in a similar way as TMP but after impregnation of chemicals to soften the wood lignin (e.g. Sundholm 1999). This thesis is mainly focusing on some aspects on wood and fibre mechanics related to the thermomechanical pulping process.

Fig. 1 shows the principle of a refiner with one rotating disc (rotor) and one stationary disc (stator). The chips are fed into the centre of the stator. Both discs are equipped with patterned segments shown in Fig. 2. The grooved pattern is coarse in the breaker bar zone towards the centre of the refiner and is finer in the refining zone towards the periphery.

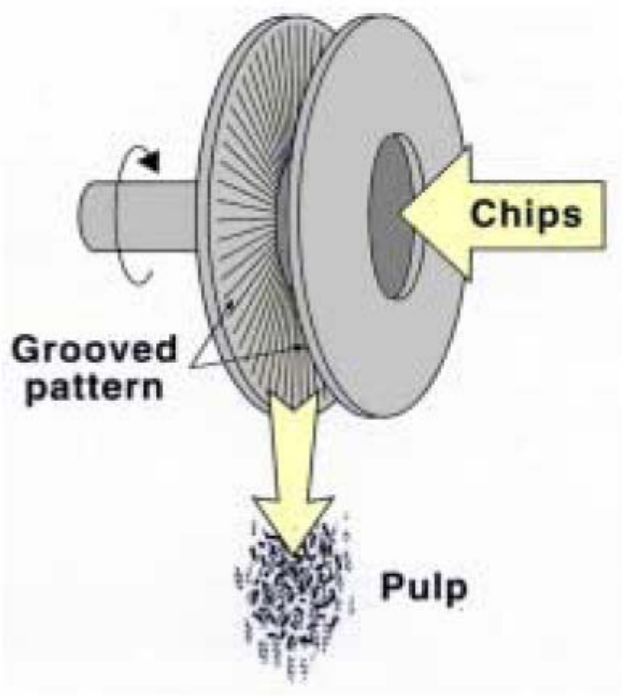

Figure 1. The principle of refining From Tienvieri et al. (1999)

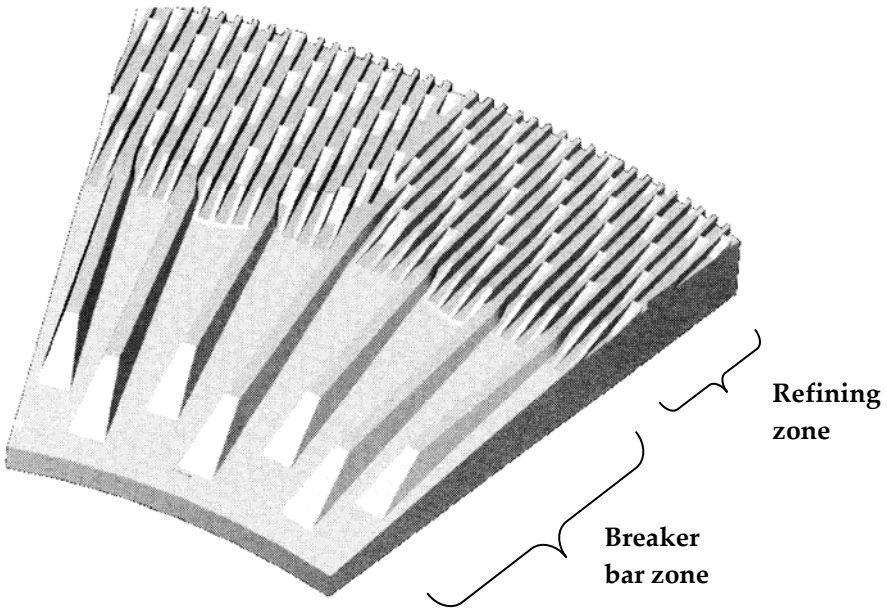

Figure 2. Typical refiner segment

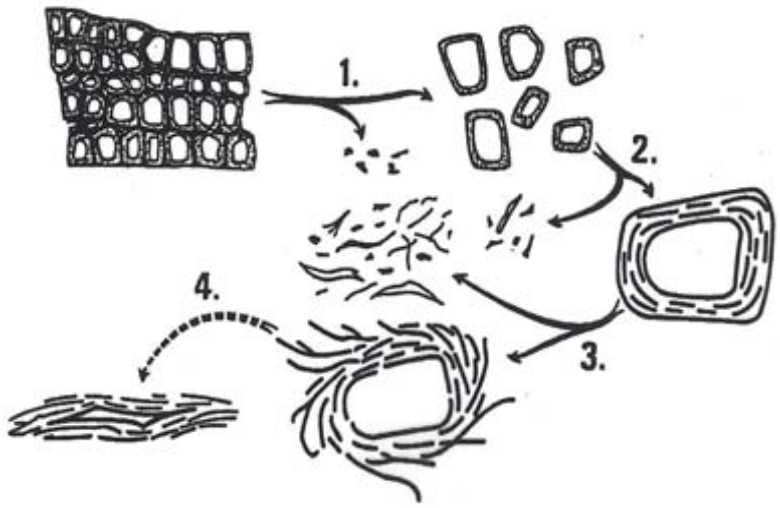

Figure 3. Hypothetical split of the chip refining process into different process stages. From Sundholm (1993).

Wood is a natural polymeric viscoelastic material and its response to mechanical treatment is greatly affected by temperature, moisture content (MC) and loading rate (e.g. Salmén and Fellers 1982). The wood chips and subsequently the fibres are subjected to a very complex deformation process in the refiner and the mechanical energy is to a large extent transformed to heat (e.g. Höglund and Tistad 1973). The wood chips are gradually broken down to smaller pieces i.e. to separate fibres, broken fibres and fines. It is likely that fatigue processes cause the fibrillation and flexibilization of fibres. Fatigue of wood will however not be discussed further in this thesis. A hypothetical split of the chip refining process into different process stages as presented by Sundholm 1993 is shown in Fig. 3.

The main wood species used for mechanical pulping is spruce but other softwoods as pine and fir are also utilized. Hardwoods as poplar, aspen and eucalyptus are also suitable for manufacturing of CTMP of special grades. Samples used in experiments reported in this thesis are all prepared from Norway spruce, *Picea abies*.

The electrical energy demand in refining to produce TMP for magazine paper grades is about 1800 to 3000 kWh/ton; newsprint grades demand about 1800 to 2200 kWh/ton and paperboard grades about 1000 to 1400 kWh/ton. Only a part of the electrical energy demand is considered to be effective in fibre separation and developing fibre properties. Therefore it is important to improve the understanding of wood and fibre mechanics related to the electric energy demanding TMP process. It is also important to improve the understanding of how this energy is distributed between the rotating plates in the refiners as separation

of fibres and developing fibre properties take place at different positions in the refiners.

1.1 General scope of investigation

The main objective of this thesis was to improve the understanding of some aspects on wood and fibre mechanics related to the conditions in the thermomechanical pulping process. Another objective was to measure the power distribution between the rotating plates in a refiner.

1.2 Outline of the thesis

A literature review aimed at describing the mechanisms at fracture in wood and fibres as related to the thermomechanical pulping process is presented in Section 2. An experimental study of fracture of wood in compression, with conditions similar to those occurring during precompression in the plug screw prior to the preheater (in some installations also prior to the refiner), is presented in Section 3. The effect of impact velocity on the fracture of wood is reported from an experimentally study in Section 4. The study is related to conditions in the breaker bar zone of the refiner plate where most of the wood is separated into single fibres. A micromechanical model of the deterioration of single wood fibres is given in Section 5. The deterioration of single fibres is related to conditions in the refining zone.

Section 6 presents measurements of the power distribution in a pilot refiner. Even though many relationships relating specific energy consumption and pulp quality have been developed over the years more has to be learned of how the supplied power is distributed within the refining zone. With this knowledge it is possible for example to improve, at least to some extent, theoretical and numerical models for the refining process.

Fig. 4 shows schematically a part of a typical TMP process. The sections corresponding to different sub processes are indicated in the figure.

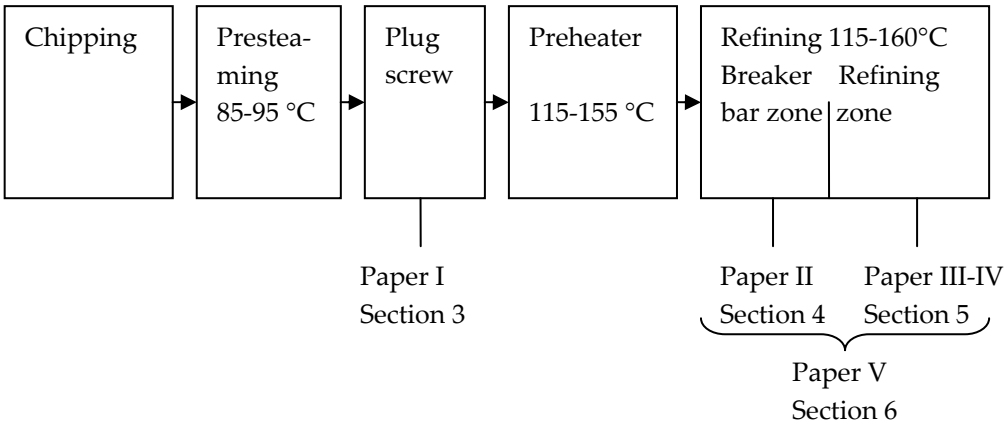

Figure 4. Part of a typical TMP process. Sections corresponding to different sub processes are indicated in the figure.

2 LITERATURE REVIEW

This literature review will start with a short description of the wood and fibre material, followed by an overview of fracture in wood and fibres related to the conditions in the thermomechanical pulping process.

2.1 The wood

Fig. 5 shows a cross-section of a softwood tree. The growth of the tree starts from the cambium, outwards to the bark and inwards to the sapwood. The hollow, longitudinally oriented cells have two purposes; to conduct liquid and to withstand mechanical loads. These so called tracheids are for simplicity just called fibres in this thesis. A minor part of the cells are radially oriented, so called ray cells. The core of the tree stem contains the heartwood where no conduction of liquid takes place. At the beginning of the growth season the soil contains good supply of nutrients which makes the fibres to grow fast. These earlywood fibres are thin-walled and somewhat larger in the radial direction compared to the thick-walled latewood fibres that are grown at the end of the season.

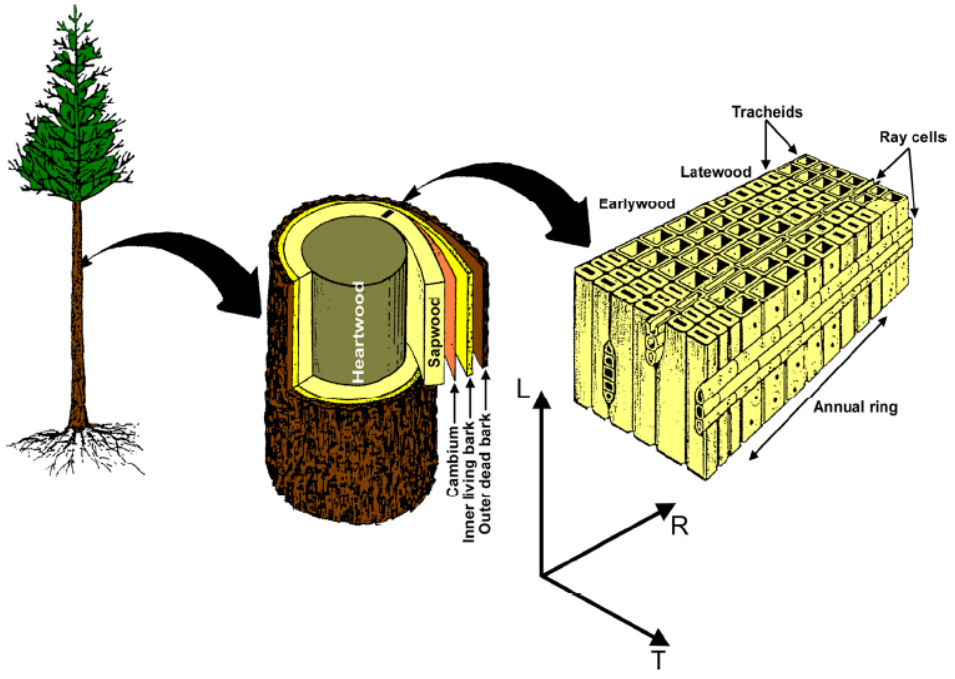

Figure 5. Schematic illustration of the morphological structure of softwood and the three principal directions of wood: longitudinal (L), radial (R), and tangential (T). From Fahlén 2005

Fibres produced during one year constitute an annual ring. Both the tree stem and the fibres have a cylindrical form. Therefore a cylindrical coordinate system is appropriate to describe the variation of physical properties along the principal directions; longitudinal (L), radial (R) and tangential (T).

2.2 The fibre material

The fibre cell wall consists of the middle lamella (ML), primary wall (P), secondary cell wall layers (S_1, S_2, S_3) and warty layer (W), as shown in Fig. 6, Côté (1967). The hollow central part is the lumen. Each cell wall layer can be considered as a composite built up by cellulose microfibrils as reinforcement in a matrix consisting of lignin and hemicelluloses. Wood is thus a natural polymeric material with viscoelastic properties. Its degree of softening and response to mechanical treatment is greatly affected by temperature, moisture content and loading rate (Goring 1963, Becker, Höglund and Tistad 1977, Irvine 1984, Salmén 1984, Kelley, Rials, and Glasser 1987, and Östberg, Salmén, and Terlecki 1990).

The degree of softening of the wood lignin, during the pre-treatment, controls where in the wood structure the rupture takes place during refining. Franzén (1986) proposed that the rupture of the fibre wall during refining takes place

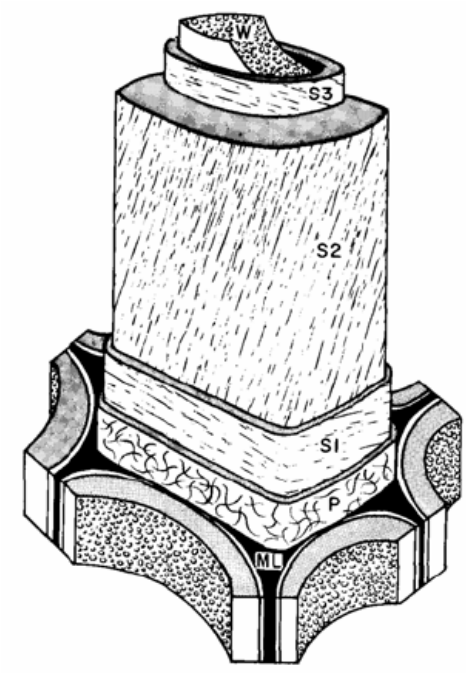

Figure 6. Simplified structure of a typical fibre cell wall. From Côté (1967)

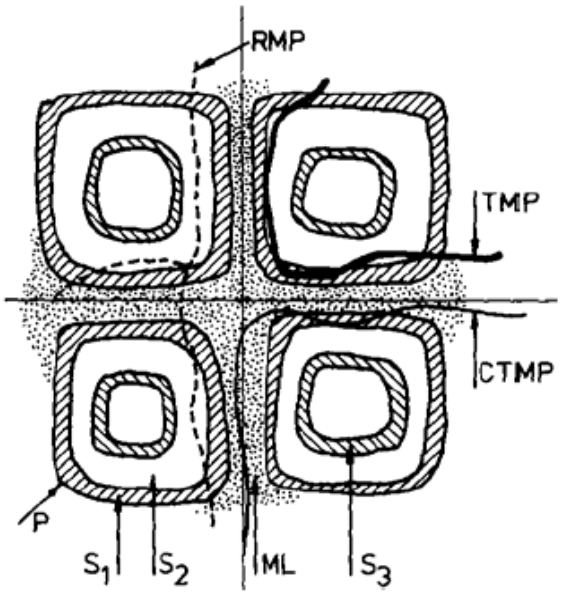

Figure 7. Typical kinds of fibre rupture in different high-yield pulping processes. From Franzén (1986)

preferentially in the primary layer (P) and in the lignin rich middle lamella (ML) if the lignin is well softened, Fig. 7. The wood fibres can be separated, with low energy input and little fibre damages, at temperatures considerably above the softening temperature of the lignin. The fractured areas become smooth and have a high fraction of lignin.

On the other hand, if the ML lignin is sufficiently stiff the separation occurs preferentially between primary and secondary walls. The lignin content in the exposed fibre surfaces will be relatively low, giving a surface that is easy to defibrillate, Atack (1972).

The softening temperature of softwood lignin and also softwood itself is about 125-145 °C at pertinent process conditions (Höglund, Sohlin and Tistad 1976, Salmén 1984, and Irvine 1985).

2.3 Wood fracture due to deformation of wood in the chipper and in plug screws

As mentioned in the introduction of this section, the wood chips are deformed even before refining. The chips are deformed both in chipping and in feeding the chips into preheaters and refiners. It is known that wood during mechanical

loading, exhibits a number of different deformation and failure phenomena e.g. plastic/viscoelastic deformation of the fibres, breaking of fibres, delamination of the fibre walls, fibre fracture and introduction of microcracks in the fibre walls (Höglund and Tistad 1973, Salmén and Fellers 1982, and Karnis 1994). Hartler (1986) proposed that the reason why compression prior to refining is a beneficial operation either could be that plastic deformations are introduced in the fibres in a more energy efficient way than in refining or that the compression leads to a more homogeneous wood mass which leads to more steady and even feeding of the refiner.

2.3.1 Deformation of wood in chipping

The basic mechanics of chip formation in disc chippers are described for example in Kivimaa and Murto (1949), and McLauchlan and Lapointe (1979). Kivimaa and Murto (1949) concluded that the extent of chip damage increased with higher spout angles and with higher sharpening angle of the knife and also with the dulling of the knife.

Stone and Nickerson (1961) and also Hartler (1963) found that longitudinal compression of fibres during chipping produces misalignments of the microfibrils in the middle layer of the secondary wall, S_2. Because of the birefringent nature of the microfibril, these deformations showed up bright against a dark background when the fibre was examined in polarised light through an analyser oriented at 90° with respect to the original polarised light and the fibre axis oriented in the extinction position.

It is also possible to show deformations in wood chipping in numerical simulations (Uhmeier 1995). He showed that a wood chipper produces chips with large parts of plastic deformation. A larger knife angle or a higher friction between wood and knife increased the extent of plastic deformation.

Also Holmberg (1998) have studied the influence of knife angle. He concluded from numerical simulations that a larger knife angle increased the energy consumption in the chipping operation and resulted in considerably more collapsed cells within the earlywood.

2.3.2 Lateral compression of wood

Salmén, Dumail and Uhmeier (1997) found that in lateral compression of wood specimens, impregnated with ethylene glycol and at temperatures up to 150°C, the weaker earlywood fibres are totally deformed before anything happens to the latewood fibres. They concluded that, in order to be energy efficient, the mechanical treatment of wood might be performed on each type of fibre separately, with only few deformations of high amplitude.

Holmberg (1998) compressed wood specimens laterally to 50% of their original thickness, at about 20°C. He found that combined radial compression and shear loading modes required about the same energy as that of pure compression compared at the same radial compression. The energy absorbed for the specimens at 28% MC was, in general, about 60% of that for the corresponding ones at 12% MC. He also observed that the collapse was localised to the earlywood fibres. Holmberg also, with rather good prediction, performed numerical simulations. A crushable foam plasticity model was used for the earlywood, the latewood was assumed to behave linear elastic and special crack elements were used between the standard solid elements.

Persson (2000) used a model based on microstructure and nonlinear material effects for a similar numerical simulation as Holmberg did. The model provided deformation results that were close to the experimental results performed at 20°C. However at strain levels about 10% and higher, numerical difficulties due to local instabilities were encountered.

Kärenlampi, Tynjälä and Ström (2003) investigated the effect of temperature and compression on the mechanical behaviour of steam-treated wood. An increase in temperature from 101 to 131°C resulted in a decrease of about 40% in the compressive stress at any particular strain up to 55%.

All of the abovementioned investigations have been conducted in servo-hydraulic testing machines. The Split Hopkinson pressure bar (SHPB) technique makes it possible to achieve high strain rates. Widehammar (2004) used this technique to investigate the stress-strain relationships for spruce wood at strain rates up to about 1000 s^{-1}. The strain rate was found to have large influence on the behaviour of the wood, especially under the condition of full saturation, where water transport in the deforming specimen is of major importance. No major damage could be seen on the fibre-saturated specimens. However the fully saturated specimens were split into small pieces at high strains when compressed in the radial and tangential directions.

Recently Holmgren et al. (2008) modified the SHPB so that experiments could be performed in steam environment. The so called Encapsulated Split Hopkinson Device (ESHD) made it possible to obtain stress vs. strain for wood specimens at high deformation rate, high temperature and high steam pressure.

Svensson et al. (2007) found, in radial and axial compression tests performed in an ESHD, that the spruce wood was more compressed due to higher strain rates at higher temperature. At 170°C they measured the strain rate 781 s^{-1} in the axial direction. They concluded that the ESHD testing technique combined with high speed photography is well suited for studying the compression of wood under conditions similar to those in a refiner.

Björkqvist et al. (1997) measured damping and propagation of shock wave in spruce sapwood specimens at temperatures up to 127°C and precompressed up to about 600 kPa. They presented the results as coefficients of elasticity and viscosity of a Voigt-Kelvin solid. The coefficients decreased with increasing temperature and the precompression had only slight effect on the coefficients.

2.3.3 Longitudinal compression of wood

Dinwoodie (1968 and 1974) made a major contribution to the present understanding of failure in wood due to longitudinal compression. He observed that small dislocations of microfibrils in the cell wall so called slip planes, progressed to grow to microscopic creases and successively to larger creases up to failure with increasing load. It was concluded that this process contributes considerably to the plastic deformation of wood compressed parallel to the grain. The appearance of dislocations was more likely to be found at parts of the tracheid, which are in contact with rays. The angle at which the slip plane traverses the cell wall was found to be a function of the angle of the microfibrils in S_2 together with the ratio of the modulus of elasticity in the longitudinal and radial planes.

Frazier and Williams (1982) precompressed wood cubes longitudinally to 35% of their original thickness and thereby reduced the required refining energy by 9% in thermomechanical pulping and by as much as 40% in chemithermomechanical pulping. From photographs they discovered that nearly every fibre was separated from the adjacent fibres by the buckling and splitting that occurred and that the separation between fibres occurred at the interface of S_1 and S_2, leaving the middle lamella largely intact and attached loosely to one fibre or the other.

Several researchers have to some extent confirmed the results by Frazier and Williams by using a screw press to study the effect of precompression (Murton 1995, Peng and Granfeldt 1996, Sabourin 1998, Johansson et al. 1999, Kure et al. 1999, and Sabourin, Aichinger and Wiseman 2003).

In the present work wood was compressed to investigate the fracture with specific emphasis on its dependence on temperature, moisture content, strain and loading direction. The wood was compressed in both the lateral and longitudinal directions in order to select preferred modes of deformation to achieve desired irreversible changes in the wood structure. Acoustic emission monitoring was carried out during compression to investigate the fracture history (Section 3).

2.4 Energy consumption in refining

How to reduce the energy consumption in thermomechanical pulping has for a long time been a key question, Atack (1981), and Sundholm (1993). A warning for the increasing energy costs was pointed out already in 1975 by Carter et al. and Pöyry (1977) called the high energy consumption "the Achilles' heel of mechanical pulp". It is therefore important to find out a theoretical value for defibration energy.

Several researchers have estimated a theoretical value for defibration energy. Campbell (1934) estimated the surface free energy to 0.6 J/m^2. Lamb (1960) found a value of defibration energy equal to about 150 J/m^2 in experiments where spruce specimens were fractured by cleavage. He explained this higher value by the viscoelastic polymers lignin and hemicelluloses and drew an analogy to the peeling of adhesive-backed tape. Also Atack et al. (1961) concluded that plastic energy was dissipated in the fracture, but since a true value of the surface area wasn't measured they were not able to give a value of the dissipated plastic energy.

In 1973 May calculated the energy to separate chips into fibres to be 10 kJ/kg (2.8 kWh/ton). Assuming the energy consumption for defibration in a real process to about 250 kWh/ton, (Marton, Tsujimoto and Eskelinen, 1981), May's calculation gives a theoretical energy efficiency of 1%.

Atalla and Wahren (1980) proposed the value 83 kJ/kg (23 kWh/ton) as an upper limit for the theoretical energy requirement for fibrillation down to diameter of 40Å. An average of 2.88 hydrogen bonds per anhydrocellobiose unit were assumed broken as a result of the partition. Nissan (1977) found the theoretical energy requirement to be about 300 kWh/ton if all impacts in a refiner led to delamination of the fibres.

Sundholm (1993) suggested that the refining efficiency is in the range of 40-60%. He pointed out that a large proportion of mechanical action is necessary to develop fibre properties. These statements were based on trials at extremely low stone speed in a pilot wood grinder.

Marton, Tsujimoto and Eskelinen (1981) divided the total energy consumption in refining into the energy used for defibration, i.e. to transform wood chips to separate fibres, E_S, and the energy used to refine the fibres for development of fibre properties, E_d, such as the energy for internal delamination, external fibrillation, improving flexibility, generating fines and cutting fibres. They found that E_S corresponds to a portion, between 9-34%, of the total energy consumed in producing a spruce TMP at a freeness of 150 ml CSF[1].

[1] Canadian Standard Freeness, CSF is a measure of pulp or stock drainability. A low value corresponds to a low drainability.

As an example; to produce a spruce TMP at a freeness of 150 ml CSF required about 2000 kWh/ton with a chip size (thickness) of 5 mm, E_S is 250 kWh/ton and E_d was 1750 kWh/ton. The value of E_d was based on refining experiments at 1% consistency with different chip sizes and the measured refining energy was extrapolated to the value for a hypothetical one-fibre chip. E_d was found to be independent of chip size. The theoretical value for defibration, E_{sth} is about 54 kJ/kg (15 kWh/ton) according to Marton, Tsujimoto and Eskelinen (1981). Depending on chip size (thickness 2-16 mm) the defibration efficiency E_{sth}/E_S was estimated to ranges from 2 to 12%. In this example the defibration efficiency E_{sth}/E_S was calculated to be equal to 6%.

The total fibre development energy, E_d was found to be about 1 150 kWh/ton to produce a spruce TMP at a freeness of 500 ml CSF. Therefore about 1/3 of E_d in their experiments was consumed in reducing the freeness from 500 to 150 ml CSF.

Marton, Tsujimoto and Eskelinen (1981) calculated the bonded surface area, of an ordinary sized spruce chip, to about 300 m^2/kg, i.e. the conversion factor from kWh/ton to J/m^2 can in this case be calculated to 12.

2.5 Wood fracture in the initial stage of refining

In the refiner, the wood chips are broken down between two discs where one or both rotate. The chips are fed in near the centre of rotation and are transported through the action of the centrifugal force towards the periphery where the pulp is discharged. In the breaker bar zone, forces are transferred to the chips, deforming and breaking them into progressively smaller pieces.

In 1973 May described this process in the following simplified way: "... chips are broken down by fracture along the grain in fairly well defined stages. They are first split into matchstick-like material, and then, as they move towards the periphery of the refining zone, into more slender pin chips, then larger fibre bundles, smaller bundles, and finally into separate fibres".

Film recordings through transparent sections of a refiner segment show that matchstick-like fragments proceed through the eye of the refiner having random orientation. In the refining zone however the major axis of the fibres and fibre bundles is oriented in a tangential direction (Atack 1980). Atack also found internal breakdown of sampled material which was about to enter the refining zone. By sampling material, through the stator in the refining zone at a number of radial locations, Atack, Stationwala and Karnis (1984) found that the reject content decreased gradually from the breaker bar section to the refiner periphery.

The size reduction of chips during refining was mathematically described by Strand and Mokvist (1989). They derived a simplified theory based on

comminution theory. The reduction of each chip size fraction was found to decline exponentially, dependent on two parameters impact intensity and wood strength.

2.5.1 Wood strength

The wood strength, expressed as energy absorption per fractured surface area, is dependent upon several factors other than the morphological ones. Some of them are fracture mode, impact direction, chip dimension, temperature, solids content and rate of deformation. In the following these factors will be commented on briefly. It should be noted that the terms wood strength, impact strength, work to failure and fracture energy often include other kinds of energy apart from pure fracture energy e.g. elastic energy, kinetic energy, plastic and viscoelastic dissipation.

Fracture mode

The three modes of fracture, shown in Fig. 8, are opening or cleavage, sliding or forward shear, and tearing or transverse shear. These are often referred to in the literature as mode I, II, and III respectively, introduced by Irwin (1958). Marton and Eskelinen (1982) concluded that defibration of chips occurs through fracture in cleavage, while the effect of refining of fibres is the result of fracture in shear, and that fracture energy in cleavage is only about a quarter of that in shear.

Impact direction

The effect of impact direction on impact energy absorption using a pendulum tester was examined by Eskelinen, Hu and Marton (1982) for eight different impact

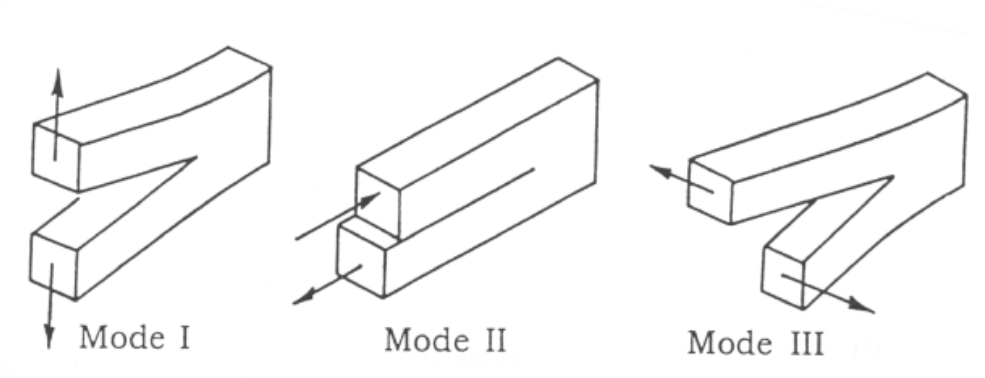

Figure 8. Definition of the three modes of fracture

direction and fracture plane combinations. The fracture always occurred along the grain, but the crack orientation in the R-T plane varied. They concluded that the impact strength was independent of the impact direction except when the crack propagated through the early/latewood transition zone. In that case the impact strength was lower than in any other case. When the crack propagated in the radial direction, from the pith outwards, smooth fracture surfaces and fewer multiple cracks were produced.

Ottestam and Salmén (2001) found that the fracture energy in the radial direction was 140 J/m^2 compared with 220 J/m^2 in the tangential direction. The explanation given was the existence of ray cells, which have to be fractured in the tangential mode, as well as the less ordered arrangement of the cells in the tangential plane.

Chip dimension

From impact tests in a pendulum tester it was found that the impact strength was a linear function of the specimen thickness or chip dimension in pure cleavage, mode I in Fig. 8 and in pure forward shear, mode II (Marton and Eskelinen 1982). The type of mode was controlled by the ratio of the specimen thickness to the tester gap (plate clearance in a refiner). If the ratio was above 2, then the fracture was said to occur in virtually pure forward shear and if the ratio was below 0.5 the fracture occurred in virtually pure cleavage. Chip size also affected the refining energy consumption. The total energy dropped by about 30% when the chip size was reduced from 16 to 3 mm (screen fractions) producing spruce TMP of 150 ml CSF. The chips were defibrated in a "Defibrator D" device at 30% consistency to 550 ml CSF and subsequently refined to about 100 ml CSF in a 30.5 cm disc refiner at 1% consistency (Marton, Tsujimoto and Eskelinen, 1981). The experiments supported their assumption that the energy for developing fibre properties was independent of the chip size.

The results by Marton, Tsujimoto and Eskelinen were confirmed by Hoekstra, Veal and Lee (1983) in a pilot-scale TMP investigation producing lodgepole pine (*Pinus contorta*). They found sizable increases in the specific energy required to reach 100 ml CSF in the 1.5 to 6 mm chip thickness range.

Hartler (1986) pointed out that thick chips are likely to be inadequately softened and can disturb chip feeding. Thick chips can also contain low quality knot wood. Therefore one has to be careful about conclusions regarding chip size and energy savings.

Temperature

A decrease in the work to failure with increasing temperature has been reported by a number of authors. Stone (1955) found the fracture energy at 130°C to be 35% of that at room temperature. Microscopic studies showed that the energy reduction was accompanied with less fibrillation of the outer surfaces. Almost the same relative reduction was found by Koran (1979) who made a thorough investigation of the temperature dependence in the range -190 to 250°C. The energy-temperature curve showed maximum fracture energy at -40°C. Ottestam and Salmén (2001) found the fracture energy at 95°C to be about 60% of that at room temperature.

Marton and Eskelinen (1982) found the impact strength-temperature relation to be dependent on the fracture mode and specimen thickness. In forward shear of 3-4 mm thick specimens, the impact strength remained almost constant up to about 110°C and then it decreased rapidly at higher temperatures up to 150°C. The impact strength in cleavage, however, decreased over the whole temperature range. These results are to some extent supported by Atack et al. (1961) who found no significant temperature effect between room temperature and 100°C.

Solids content

The impact strength - solids content relation was also found to be dependent on the fracture mode (Marton and Eskelinen 1982). An increase in solids content from 30% to 45% decreased the impact strength in mixed (I and II) mode slightly but increased the impact strength in forward shear by approximately 50%.

This result is important for high-consistency refining with inlet consistencies typically between 18-30% (Miles and May, 1990) and outlet consistencies between 40-50% (Sundholm, 1999).

Rate of deformation

Atack et al. (1961) found a decrease in fracture energy from 100 to 70 J/m^2 when the rate of deformation was increased from $2 \cdot 10^{-4}$ to $2 \cdot 10^{-3}$ s^{-1}. The tests were performed at room temperature and the samples were cracked prior to testing. On the contrary, Marton and Eskelinen (1982) found an increase in impact strength with increased shear rate. The effect was more pronounced with thin specimens. The shear rate was varied between 550 to 11.000 s^{-1} by varying the tester gap in a pendulum tester with a constant impact velocity of 1.65 m/s. From this they concluded that an increase in the "severity of impact" by refining through decreased plate gap or increased rotational speed does not necessarily reduce energy consumption. Holmberg (1996) also found an increase in fracture energy

with higher strain rates. An increase in strain rate from $3.3 \cdot 10^{-4}$ to 3.3 s^{-1} resulted in an increase in fracture energy from 170 to 380 J/m^2.

The results of Atack et al. seem to contradict those of Marton and Eskelinen, and Holmberg though the differences in the rates of deformation used were considerable. Therefore further research into the effect of impact velocity on the fracture energy would be of great interest.

2.6 Wood fracture energies measured by different researchers

The fracture energy or work to failure of spruce wood samples has been presented by a number of workers. The measured fracture energies, E_f, of these tests are summarised in Table 1. All specimens were water saturated or in green condition and the tests were conducted at room temperature. Some values are extrapolated to small dimensions and are close to the theoretical defibration energy, E_{sth}, as explained by Marton, Tsujimoto and Eskelinen (1981) and Eskelinen, Hu and Marton (1982) [cf. Section 2.4].

When the samples have an initial crack (notched samples) it appears that the tests are less sensitive to the sample dimensions and therefore there is no need for extrapolation to small dimensions. According to Marton and Eskelinen (1982) the fracture energy in forward shear of spruce is 340 J/m^2 compared to 170 J/m^2 in cleavage as obtained by Eskelinen, Hu and Marton (1982). Fracture energy of 180 J/m^2 was obtained by Marton, Tsujimoto and Eskelinen (1981) in refining experiments which implies that defibration of chips preferable occurs through fracture in cleavage.

The data reported in the literature on the dependence of impact velocity on the wood strength are to some extent contradictory and there are few reported impact velocities above 1.65 m/s. The present work is therefore focused on fibre separation and specifically the effect of impact velocity on the fracture energy. The generated surfaces are also examined under microscope (Section 4).

Table 1. Fracture energies of spruce wood samples measured by different researchers.

a) Tensile tests on notched samples
b) The value is extrapolated to small dimensions and is close to the theoretical defibration energy as explained by Marton and Eskelinen (1982), and Eskelinen, Hu and Marton (1982).

Fracture surface dimension	**Loading rate, m/s**	**Fracture mode**	E_f **J/m2**	**Reference**
38.1 x 6.4 mm^2	167 x 10^{-6}	Cleavage [a]	100	Atack et al. (1961)
5.25 mm (thickness)	1.65	Cleavage	1400	Eskelinen, Hu and Marton (1982)
		Cleavage	170 [b]	Eskelinen, Hu and Marton (1982)
20 x 10 mm^2	10x10^{-3}	Cleavage[a]	380	Holmberg (1996)
4 x 10 mm^2	33 x10^{-6}	Cleavage [a]	140-220	Ottestam and Salmén (2001)
0.12 mm (thickness)		Transverse shear	120	Lamb (1960)
4.0 mm (thickness)	1.65	Forward shear	1800	Marton and Eskelinen (1982)
	1.65	Forward shear	340 [b]	Marton and Eskelinen (1982)
5.0 mm (thickness)		Refining experiments	1100	Marton, Tsujimoto and Eskelinen (1981)
0.252 mm^2		Refining experiments	180 [b]	Marton, Tsujimoto and Eskelinen (1981)

2.7 Impact intensity

2.7.1 Impact intensity in the initial fibre separation

Falk, Jackson and Danielsson (1987) found that the primary stage is largely responsible for establishing the characteristic properties of the pulp. In a comparison between double disc and single disc primary refiner they found that the double disc as a primary refiner produced pulp having lower specific energy consumption to a given freeness level, with improved density, light scattering and sheet surface characteristics, however with reduced tear strength characteristics.

Findings e.g. by Heikkurinen, Vaarasalo and Karnis (1993) have shown that it is the initial fibre separation step in refiner mechanical pulping that is crucial in determining how efficiently the energy is applied to the wood material. They analysed coarse pulp samples produced at low energy inputs varying refining temperature and rotational speed. They concluded that changing the refining intensity in the second-stage refiner does not affect properties as light scattering and tensile strength.

Also Höglund et al. (1995) understood the importance of impact intensity in the initial fibre separation. In the Thermopulp process they optimised the energy split between the primary and secondary stage refiner with respect to minimise the energy consumption maintaining pulp properties. With an energy input of 600 kWh/ton in the primary stage, at a temperature close to the softening temperature of lignin and an energy input of 1050 kWh/ton in the secondary stage, at a temperature well above the softening temperature, they achieved energy savings of about 20% in pilot trials producing TMP at 150 ml CSF.

2.7.2 Impact intensity in refining

The average impact intensity or the refining intensity was defined by Miles (1990) by two different numbers, the average specific energy per impact $e = E/n$ and the specific refining power $\acute{e} = E/t$, where n is the total number of bar impacts and t is the residence time. At a given specific energy, the pulp quality was found to be strongly related to the calculated refining intensity. Freeness, bulk, and tensile strength were controlled by e, whereas rejects, fibre length, and opacity were linked to $\acute{e}$. The refining intensity was calculated utilising a simplified algebraic formula, and was found to be inversely proportional to the pulp inlet consistency but insensitive to the specific energy, E, applied.

The dependence on rotational speed was quadratic and cubic for e and $\acute{e}$ respectively, and the dependence on disc diameter was linear and quadratic for e and $\acute{e}$ respectively (Miles 1991). Sundholm, Heikkurinen and Mannström (1988) found that by increasing the rotational speed from 1500 to 1800-2000 rpm it was possible to reduce the energy consumption by 5% without any drop in tear

strength. A probable explanation to this was given as an increase in "impulse moment of the bars".

2.7.3 Residence time

Ouellet et al. (1996) used black dyed and bleached pulp to measure the residence time in a laboratory disc refiner. Change in reflectance was measured as the dyed pulp passed fibre optic probes positioned around the inner and outer radii.

A method to measure the residence time of fibre in a single disc refiner by means of a radioactive tracer material was presented by Härkönen and Tienvieri (1995) and Härkönen, Huusari and Ravila (1999). The method was reported to be technically fairly simple and straightforward but time laborious. Interesting results from measurements in high consistency refiners, using this radioactive method, were reported by Härkönen, Kortelainen and Virtanen (2003). The fibre residence time in the primary stage was found to decrease with lower consistency and pressure drop and with higher production rate.

2.8 Fibre fracture in refining

During refining, a partial collapse of the fibre is desirable as well as a rupturing and reduction of the fibre wall thickness. In the refiner the fibres are subjected to lateral compression, tension and shear which causes the creation of microcracks in the fibre wall (Hattula and Mannström 1981, Mohlin 1997, Hamad and Provan 1995). This damage reduces the fibre wall stiffness and increases the surface area, which makes the fibre more conformable (Paavilainen 1993) and enhances the formation of a stronger and smoother paper, with improved runnability and printing quality. The increase in surface area also adds opacity (Rundlöf et al. 1995). A discussion of the fibre development during mechanical pulp refining can be found in e.g. Karnis (1994), Mohlin (1997), Kure (1997), and Reme, Johnsen and Helle (1999).

Kure (1997) studied the development of structural fibre dimensions in the first stage in a 36" pilot scale double disc refiner. He found that earlywood fibres with large lumen perimeters seemed to be more frequently ruptured and broken down compared to latewood fibres during refining. The latewood fibres with thick fibre walls were subjected to extensive peeling of material from the fibre surface.

Tchepel et al. (2003) concluded, from pilot-scale trials, that changes in flexibility of long fibres as a result of refining are primarily determined by changes in cross-sectional dimensions of the fibre rather than their elastic modulus.

For a given fibre transverse dimensions, fibres with low microfibril angles offer less resistance to transverse collapse than fibres with high microfibril angles (Jang et al. 2002).

The stress distribution in each layer of the cell wall of deformed fibres was studied, by two-dimensional analysis by Mark (1967), Schniewind and Barret (1969), Mark and Gillis (1970), and Schniewind (1970). Studies were extended to three dimensions by Tang (1972), Tang and Hsu (1973) and Gillis and Mark (1973). The latter studies made it possible to predict the radial distribution of stress induced by an axial force. However, the analyses were restricted to simplified geometries and boundary conditions. Finite element simulations were performed by Barrett and Schniewind (1973) and Thorpe and McLean (1983). The introduction of three-dimensional finite element simulations facilitated the application of more realistic geometries and boundary conditions. Bergander and Salmén (2002) modelled the influence and magnitude of variations of microfibril angle and layer thickness on fibre cell wall properties. The influence of S_2 layer was found to be dominant, but the S_1 layer also contributed to a certain extent to properties of the transverse direction.

The microstructural degradation in fibre cell walls being subjected to cyclic mechanical action has been studied with a single-fibre tensiometer in conjunction with a confocal laser scanning microscope by Hamad and Provan (1995). They found that cyclic shear, relative to radial compression and tension, was the most significant mode of loading to develop macro-cracks, slip planes, and micro-compressions in fibre cell walls.

The present work comprises a simple two-dimensional analytical model together with an energy criterion which makes it possible to predict the stiffness degradation and the damage state in a wood fibre, loaded in uniaxial tension or shear (Section 5).

3 WOOD FRACTURE DUE TO COMPRESSION (PAPER I)

The effect of temperature on fracture of wood in compression was investigated by use of acoustic emission monitoring. The wood was compressed in both lateral and longitudinal directions to produce preferred modes of deformation in order to achieve desired irreversible changes in the wood structure. The purpose was to simulate the effect of feeding of chips into preheaters and refiners.

Acoustic emission (AE) is a phenomenon in which stress waves are emitted from a rapid, localised change of strain energy in a material, meaning that e.g. flaws, which are created in the material, can be detected. By detecting the AE with a sensor and amplifying the signal it is possible to define an AE event by its energy content, peak amplitude, duration etc.

DeBaise, Porter and Pentoney (1966) were first to use AE monitoring during compressive longitudinal loading of wood. They observed very low emission densities, 0.001-0.02 events/cm^3 at failure in compression compared to approximately 10^4 events/cm^3 in tension. This result confirmed their expectation that compressive load was closing intrinsic flaws in the material. A more thorough introduction to and literature review of AE on wood can be found in e.g. Ansell (1982), and Kawamoto and Williams (2002).

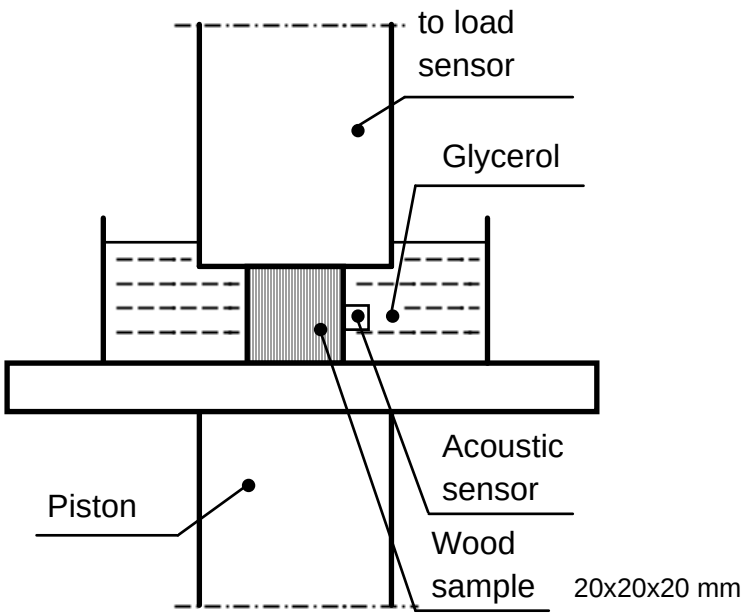

Figure 9. Schematic drawing of the experimental setup showing the testing machine and the acoustic sensor

3.1 Experimental

Glycerol was used as an impregnation liquid in order to heat the wood up to 180 °C. Glycerol was selected because it possesses a high boiling point (290°C) and has similar physical properties to those of water (Koran 1979, and Dumail and Salmén 1997). Thus the use of glycerol enabled testing above the boiling point of water, without the need to develop a rather complicated pressurised conditioning chamber.

The samples were positioned in the testing machine and an acoustic sensor was attached to the wood sample, as shown in Fig. 9.

3.2 Results and discussion

Typical curves from one of the compression tests of wood samples are shown in Fig. 10.

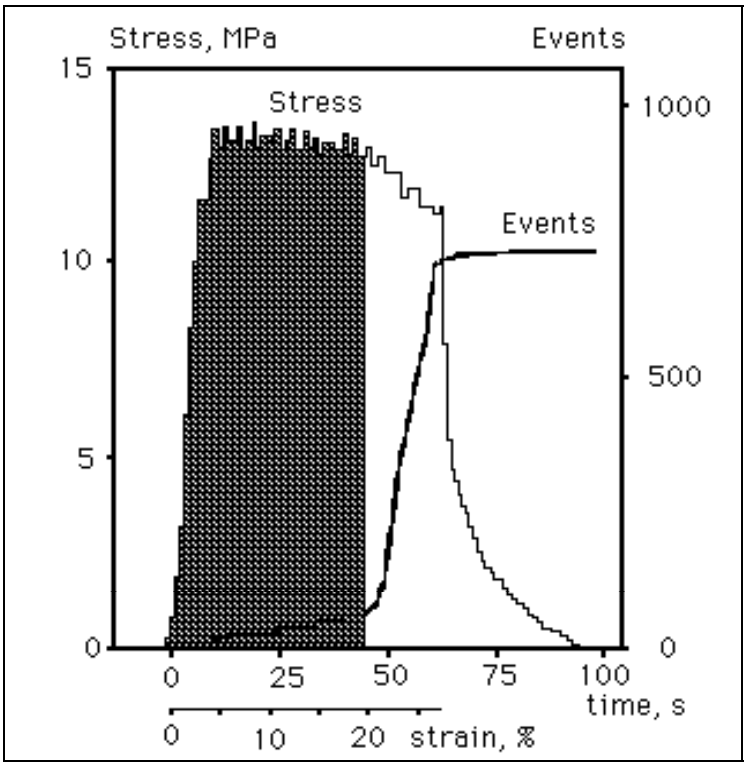

Figure 10. Average compressive stress and cumulative emissions versus time. Longitudinal compression, 50% solids content, 22°C

The compressive stress and the cumulative AE events are both plotted versus time, which is easily translated to displacement as the crosshead speed is constant at 0.1 mm/s. The maximum stress of 13.4 MPa in the example was achieved at about 4% compression and remains relatively constant up to about 20% strain where the sample is split. It is at this point that substantial AE is achieved. The unloading starts at an average strain of 27% where the cumulative AE reaches 720 events. As can be seen, it is almost silent during unloading. The reason is that generation of AE occurs during plastic deformation and must intrinsically arise from dynamic microcracking. The shadowed area is proportional to the compressive work done before onset of substantial AE.

Values based on nine tests at room temperature and at 50% solids content show that a longitudinal compression of 24% and an energy input of 3 kWh/ton is needed in order to achieve substantial AE.

A typical distribution of number of events by peak amplitude is shown in Fig. 11. A maximum is found at 26-28 dB_{AE} and at higher amplitudes the number of events decreases exponentially. There are almost no counts above 46 dB_{AE}. This exponential decline can be described by a constant *b*, which is characteristic of a certain type of failure. The constant *b* is defined as the negative slope of the distribution of number of events by peak amplitude in a log-log plot (Pollock 1981).

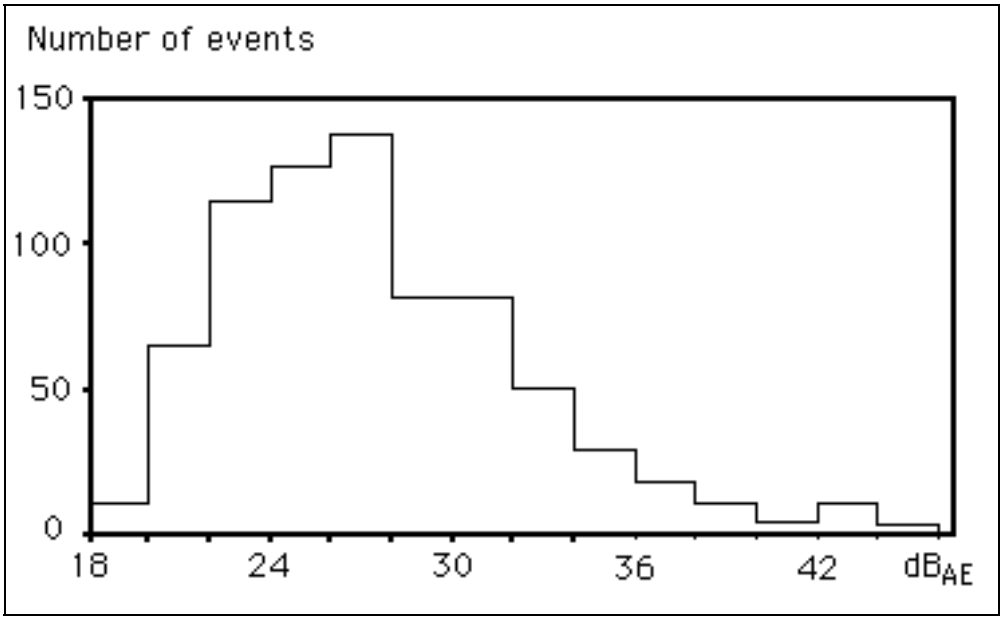

Figure 11. Distribution of number of events by peak amplitude

The factor *b* was calculated to 1.4 on average at room temperature and there was no significant dependence on solids content. From SEM-photopgraphs [cf. Paper I, Fig. 11] it can be concluded that the type of failure that predominates is the separation of rows of fibres from adjacent rows of fibres. A similar failure mechanism was also found by Frazier and Williams (1992) and Sabourin, Aichinger and Wiseman (2003). For translaminar shear, before failure in a wood laminate, *b* was calculated to 1.2 by Pollock (1981).

The dependency of number of events on temperature, at a total strain of 20%, is shown in Fig. 12. The total number of events decreases from 500 to 20 events/cm^3, for the glycerol-impregnated samples, when the temperature was increased from 23 to 120°C. One explanation is that the wood would rather flow at high temperatures when loaded in compression than to create flaws and to defibrate. A further increase in temperature to 180°C results in about 8 events/cm^3.

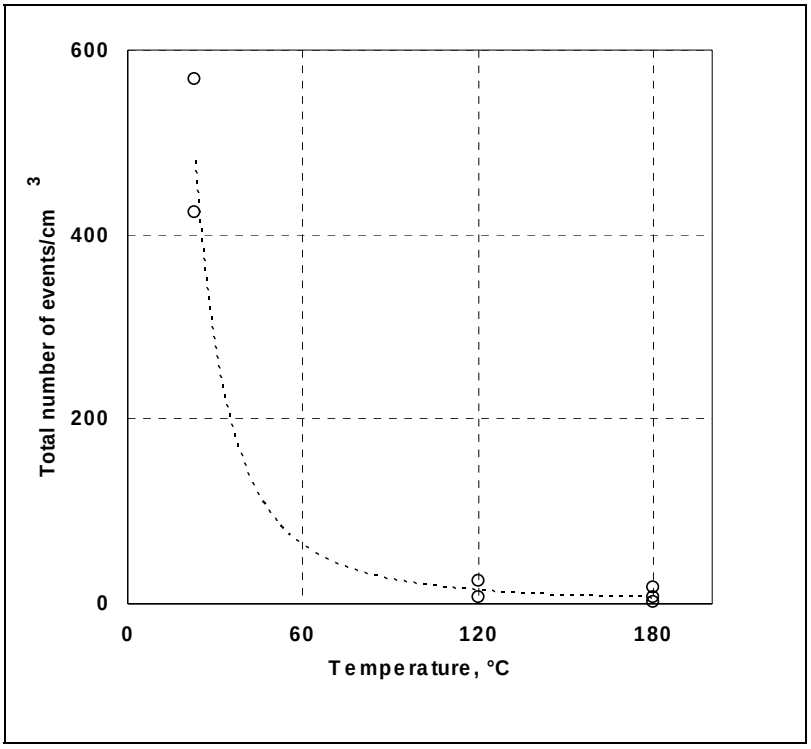

Figure 12. Total number of events versus temperature at a total strain level of 20%, longitudinal compression

Obviously, our experiments show that the compression should be carried out at temperatures well below 120°C to introduce failure sites in the wood.

As can be seen in Fig. 13 there are more AE counts when the samples are subjected to longitudinal compression, 600 events/cm^3 as a mean value, compared to 30 events/cm^3 in radial and tangential compression.

Thus, the most efficient loading direction is longitudinal in order to introduce flaws in wood under compression.

The effect of solids content on AE counts was not possible to establish in the present study.

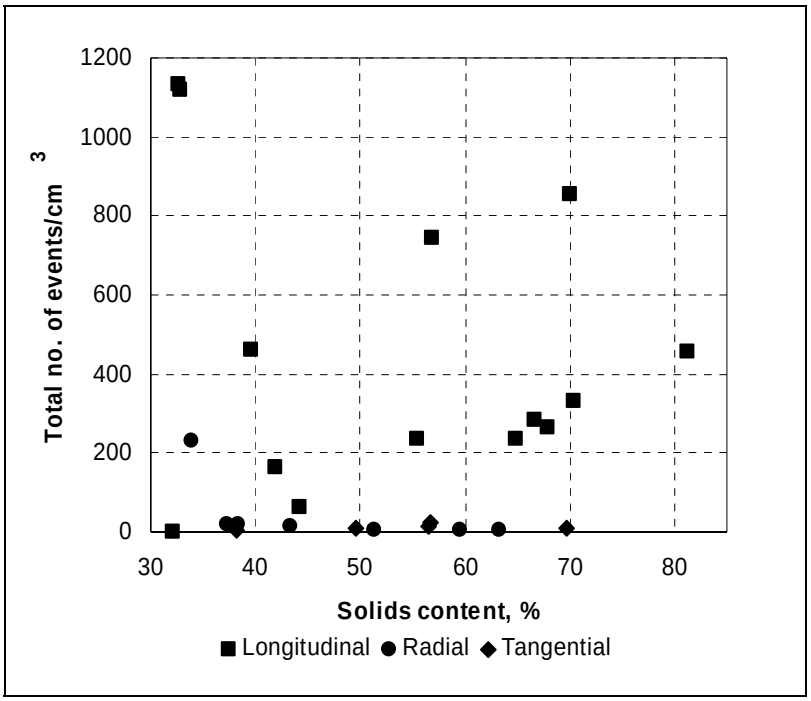

Figure 13. Total number of events versus solids content at a total strain level of 33%, 23°C

3.3 Conclusions

To achieve substantial changes in the wood structure during feeding of chips into preheaters and refiners, it is crucial that:

- the wood is compressed in the longitudinal direction;
- the compression is carried out at temperatures well below 120°C; and
- the longitudinal compression should be carried out to at least about 20%, corresponding to a specific energy input of 3 kWh/ton.

4 WOOD FRACTURE IN REFINING (PAPER II)

The fibre separation step and specifically the effect of impact velocity on the fracture energy were studied by use of a falling weight impact tester. The generated fracture surfaces were also examined under a scanning electron microscope.

4.1 Experimental

In this experimental study, the impact velocity, v, was varied between 2.5 to 5 m/s and the tests were performed at room temperature. The experimental setup is schematically shown in Fig. 14. The gap, h, can be varied to obtain different strain rates, v/h, at the same impact velocity. The sample thickness, d, was varied between 2 - 5 mm and the free specimen length, l_f, was held constant at 8 mm.

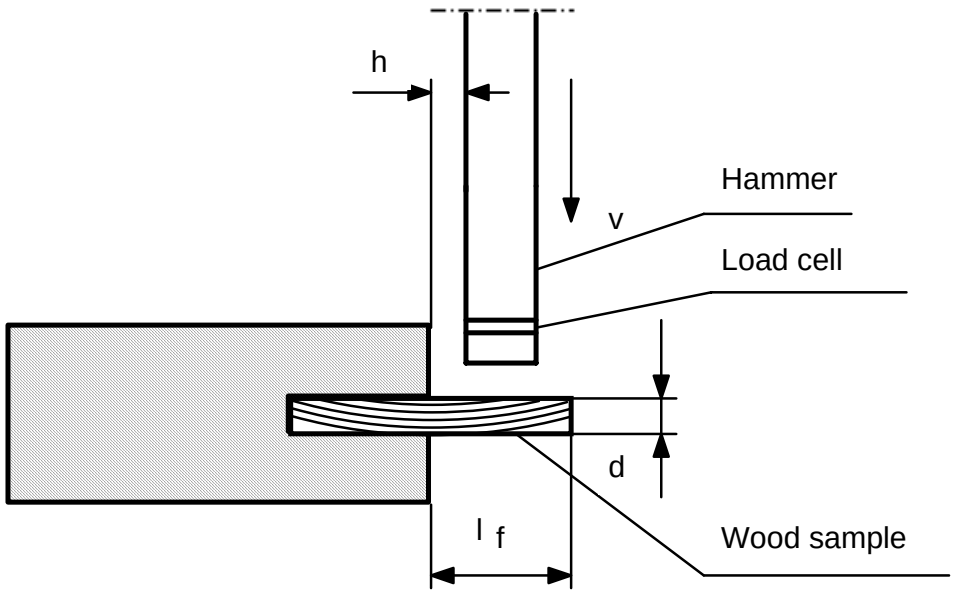

Figure 14. Schematic drawing of experimental setup. The impact direction was radial and the normal to the fracture surface was parallel to the tangential direction. The falling weight velocity v, the gap h, the sample thickness d and the free length l_f are indicated in the figure.

As stated in the literature review, when the crack propagates in the radial direction, from the pith outwards, smooth fracture surfaces and fewer multiple cracks are produced (Eskelinen, Hu and Marton 1982). Therefore this direction was chosen in the present study. The three principal directions of wood: longitudinal, radial, and tangential are defined in Section 2.1, Fig. 5.

A typical signal from the load cell during the impact together with the integrated signal, i.e. the impact energy, is shown in Fig. 15. In a numerical study carried out by Holmberg (1996) a similar general appearance of the signal was shown. He concluded that the response was non-smooth since it contained high frequent components, due to vibrations of the wood sample.

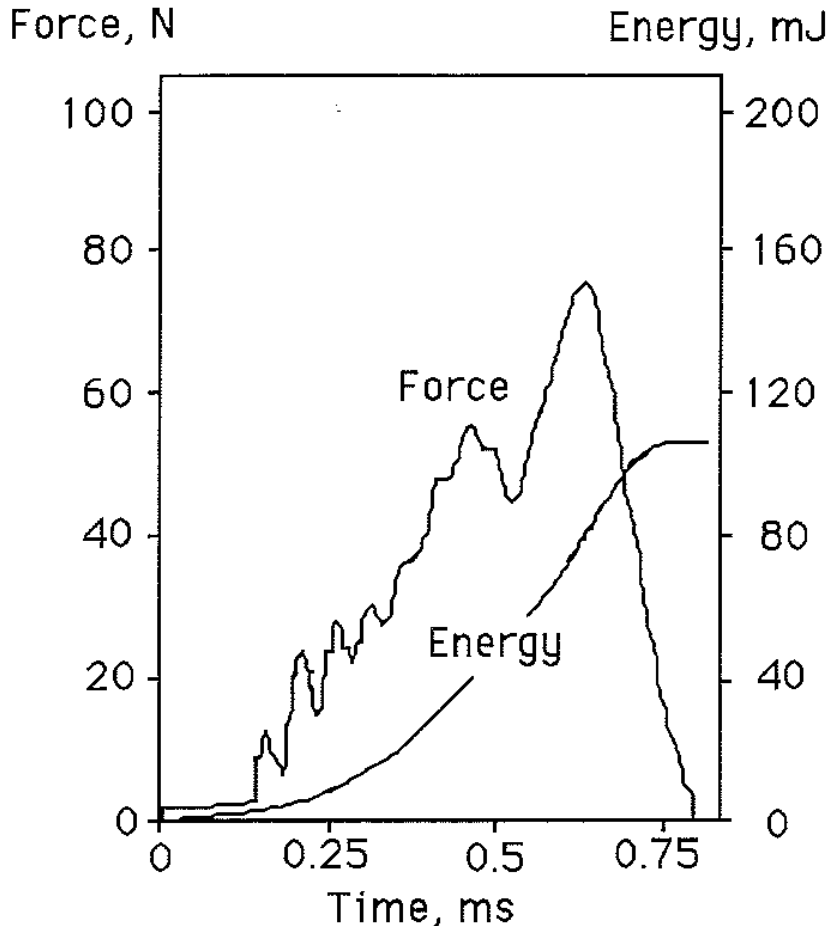

Figure 15. A typical signal from the load cell together with the integrated impact energy

4.2 Results

Two levels of impact strength, evaluated at a 3.0 mm sample thickness, i.e. 1.3 kJ/m^2 at 2.7 m/s and 1.9 kJ/m^2 at 4.8 m/s are shown in Fig. 16. This implies that impact strength increase with about 50% with the increased impact velocity. Regression lines are fitted to the data with the assumption of a Weibull distribution and scatter bandwidths, with a confidence level of 80%, are indicated in the figure. The statistical calculations follow those in Gamstedt (1995).

One explanation for the increase in impact strength with increased impact velocity is that the fracture is more shear-dominated at higher velocities due to inertia forces. According to Marton and Eskelinen (1982) the fracture energy in forward shear of spruce is 340 J/m^2 compared to 170 J/m^2 in cleavage as obtained by Eskelinen, Hu and Marton (1982) [cf. Section 2.6, Table 1]. Another explanation is an increase in kinetic energy in the wood sample.

These two explanations were both verified and quantified by finite element simulations carried out by Holmberg (1996). The simulations were incorporated and done parallel with this experimental study.

Holmberg (1996) showed that an increase in impact velocity from 2.5 to 5 m/s resulted in 20% higher impact strength. This was mainly explained by an increase

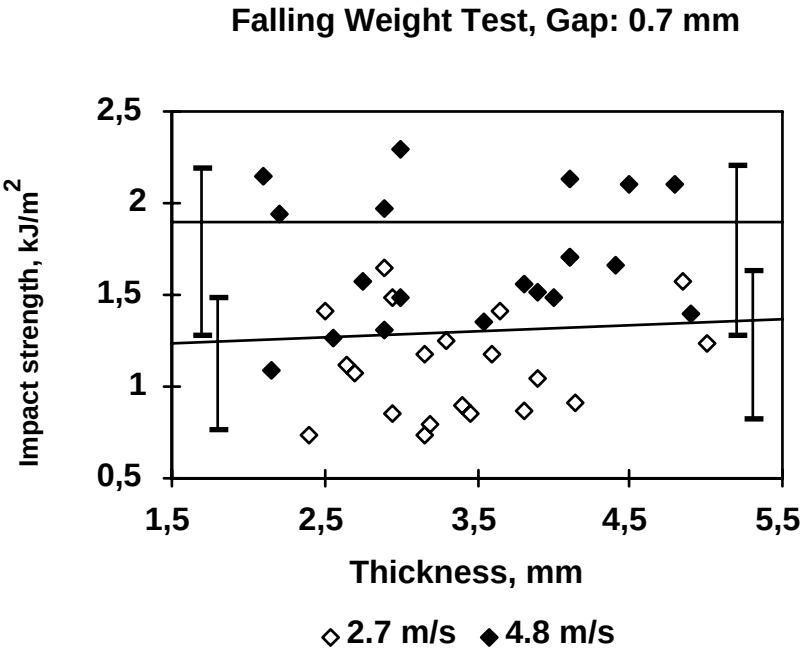

Figure 16. Impact strength vs. specimen thickness at a tester gap of 0.7 mm

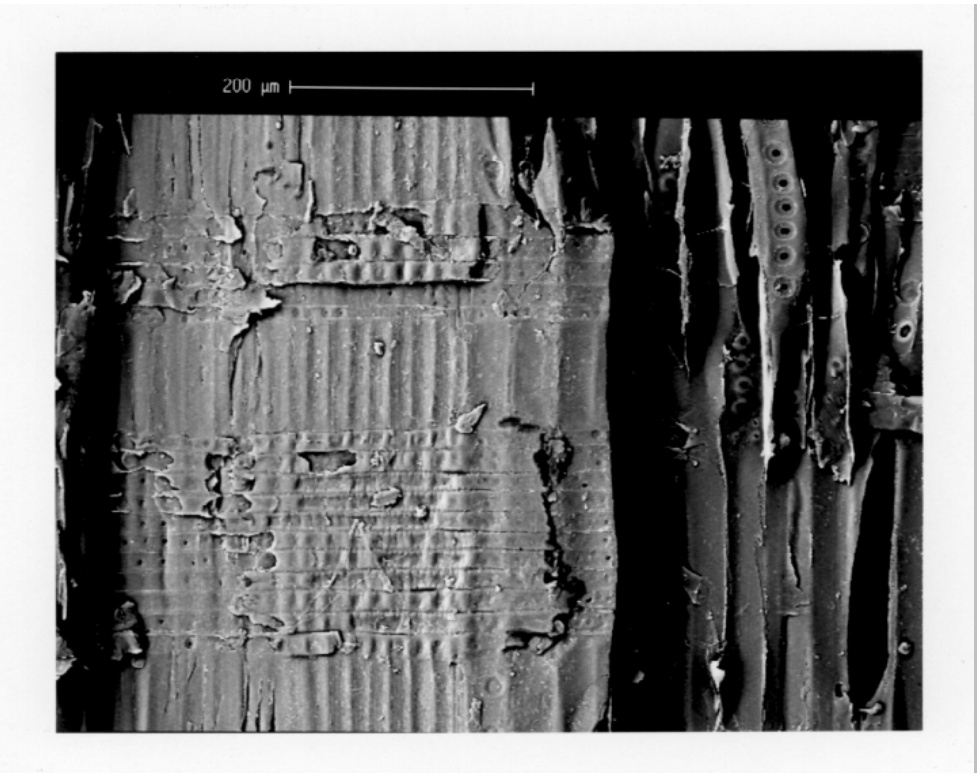

Figure 17. SEM photograph of a typical fracture surface showing zones of intact latewood fibres, to the left, and zones of broken earlywood fibres, to the right. Photo by S. Palovaara, SCA

in kinetic energy and a more shear-dominated fracture. The kinetic energy increased by a factor 2.8 and the fracture energy increased by 7%.

Microphotographs of the fracture surfaces of the wood samples indicate that there are zones of intact fibres as well as zones of broken fibres. At fracture in areas with latewood fibres, separation occurs mostly in the middle lammelae. The earlywood is mostly fractured through the cell walls, as can be seen in Fig. 17.

A third possible explanation for the impact strength - velocity relation is therefore that a higher impact velocity produces more broken fibres and thereby a higher impact energy. This can also explain the difference in impact strength between the experiments and what is predicted by the numerical studies.

4.3 Conclusions

- The experiments show that an increase in impact velocity from 2.7 to 4.8 m/s increases the impact strength by about 50%.
- The increase in impact strength with increased velocity is explained by a more shear-dominated fracture together with an increase in kinetic energy.

5 FIBRE FRACTURE IN REFINING (PAPER III AND IV)

In the thermomechanical pulping process the individual fibres are subjected to lateral compression, tension and shear which causes the creation of microcracks in the fibre wall. This damage reduces the fibre wall stiffness and increases the surface area which makes the fibre more conformable and enhances the formation of a stronger and smoother paper, with improved runnability and printing quality.

A simplified analytical model is presented in this section for the prediction of the stiffness degradation and the damage state in a wood fibre, loaded in uni-axial tension or shear. The model that is presented is based on an assumed displacement field together with the minimum total potential energy theorem. For the damage development an energy criterion is employed. The model is applied to a specific example and the relevant stiffness coefficients are calculated as a function of the damage state. The damage development as a function of the applied loads is also given.

5.1 Analytical model

The fibre cell wall model is composed of five layers [cf. Section 2.2, Fig. 6]. The layers are the primary wall (P) and the outer, middle and inner secondary walls (S_1, S_2 and S_3). The fibres are connected to each other in the wood by the middle lamella (ML), which is also considered as a part of the fibre in the analytical model.

Each layer is considered as a composite. The matrix is formed of a mixture of lignin and hemicelluloses and the reinforcing components, the microfibrils, are consisting of crystalline cellulose.

The microfibril angle, the thickness of each layer and the mass of cellulose, hemicelluloses and lignin are given as input material parameters. The elastic properties of the fibre cell wall components are also given with respect to their principle axes.

The loading cases that should be considered are illustrated in Fig. 18a, where σ_{e0} and τ_{e0} are the applied tensile and shear external bulk stresses. With reference to Fig. 18b, it is assumed that during loading of the fibre, equally spaced cracks will appear in S_2 and S_3 and running parallel to the microfibrils in S_2.

The inner cell wall layer in the model depicted in Fig. 18c, with thickness t_1 consists of S_2 and S_3 which are combined. The dominant middle secondary wall S_2 is reinforced by microfibrils, running at a certain angle α, with respect to the axial direction of the fibre. The outer layer, with thickness t_2 consists of ML, P, S_{1+} and S_{1-} combined to one layer. Both the inner and outer layer are assumed to be linear elastic and anisotropic with its relevant in-plane elastic constants obtained from lamination theory.

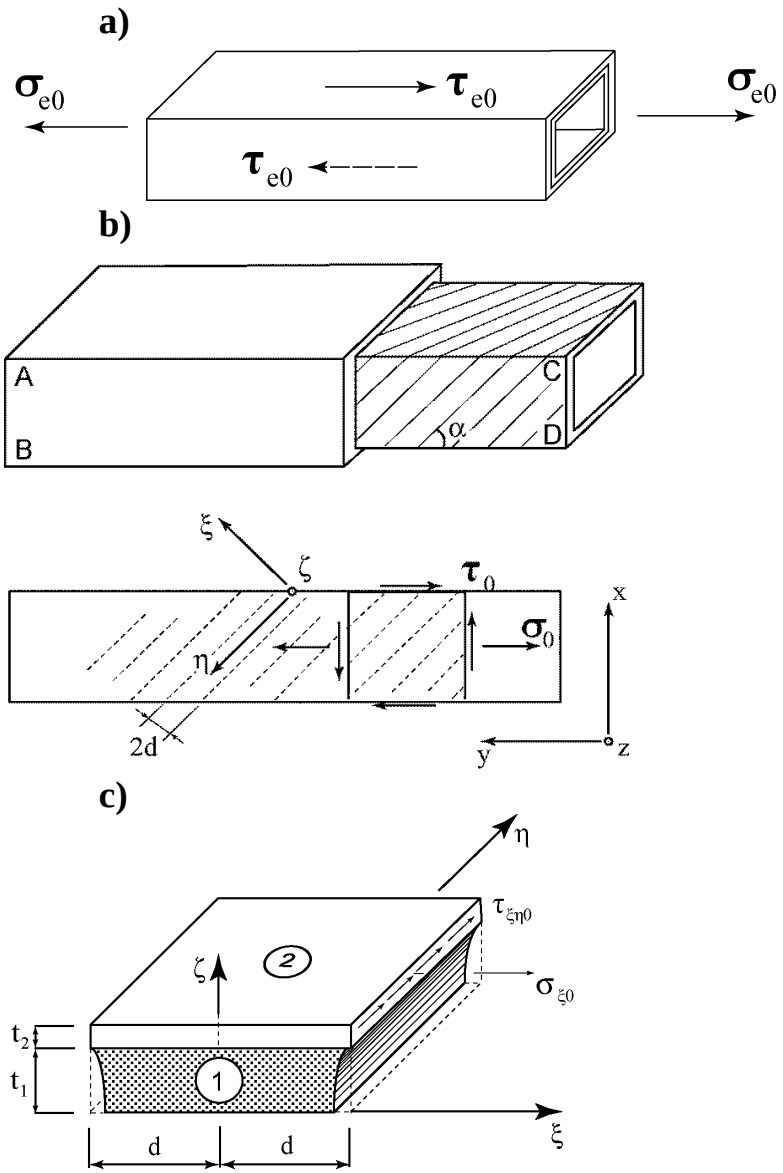

Figure 18. a) Loading cases; σ_{e0} and τ_{e0} are the applied tensile and shear external bulk stresses; b) Cracking of a fibre; Equally spaced cracks will appear in S_2 and S_3 and running parallel to the microfibrils in S_2, which are aligned at a certain angle α, with respect to the axial direction of the fibre. σ_0 and τ_0 are the external bulk stresses in a fibre wall, ACDB; c) Unit cell; $\sigma_{\xi 0}$ and $\tau_{\xi\eta 0}$ are statically equivalent to the external bulk stresses σ_0 and τ_0.

For the damage development it is assumed that the damage will increase, when the stored elastic strain energy in the wood fibre corresponds exactly to the amount of energy consumed when the crack distance $2d$ is halved. This assumption is certainly arguable, but it is adopted here due to its simplicity. The damage D_S is defined as:

$$D_S = t/d \tag{1}$$

where t is the fibre wall thickness, ($t = t_1 + t_2$ in Fig. 18c)

It is now assumed, that in the local coordinate system ξ–ζ–η the deformations will be independent of η. The model to be considered or as it will be referred to, the unit cell, is shown in Fig. 18c with its sides aligned with the local coordinate directions.

On the uncracked boundary, which is assumed to remain plane during loading, the unit cell is loaded by stresses, having average values $\sigma_{\xi 0}$ and $\tau_{\xi\eta 0}$ that are statically equivalent to the external bulk stresses σ_0 and τ_0.

The initial damage state D_{S0} and the energy consumed when creating one unit of crack surface i.e. the specific fracture energy G_C, appear as input parameters in the model.

Output from the model is the apparent E-modulus E_{app}, the apparent shear modulus G_{app}, the tensile bulk stress σ_0 and the shear bulk stress τ_0 all as a function of the damage state or number of crack distance divisions j, as described in Paper III.

The stress-strain curves can be derived by an iterative procedure assuming unloaded initial conditions, Eqs. 2 a-c and 3 a-c for loading in tensile and shear respectively.

$$\varepsilon_{0,0} = 0 \tag{2a}$$
$$\sigma_{0,0} = 0 \tag{2b}$$
$$\varepsilon_{0,j} = \varepsilon_{0,j-1} + (\sigma_{0,j} - \sigma_{0,j-1})/E_{app,j} \tag{2c}$$

$$\gamma_{0,0} = 0 \tag{3a}$$
$$\tau_{0,0} = 0 \tag{3b}$$
$$\gamma_{0,j} = \gamma_{0,j-1} + (\tau_{0,j} - \tau_{0,j-1})/G_{app,j} \tag{3c}$$

A detailed derivation, of the expressions for the elastic fields in the unit cell, is given in Paper III.

Eq. 27 in Paper III was unfortunately incorrect. It should read:

$$\sigma_{\xi}^{*} = \sigma_0 \sin^2 \alpha + 2\tau_0 \sin\alpha \cos\alpha$$

$$\tau_{\xi\eta}^{*} = \tau_0 \cos(2\alpha) + \frac{\sigma_0}{2}\sin(2\alpha)$$

Consequently are also Table V and Figs. 7-8 in Paper III incorrect. These are however corrected in the following section.

5.2 Numerical example

In the following a numerical example is presented to show the utility of the analytical model. The particular fibre to be studied is a spruce fibre with data typical for latewood and earlywood as given in Tables 2 and 3. The elastic properties of the cell wall components at 12% moisture content (MC) and 20°C were chosen as the averages of the highest and lowest stiffness coefficients of each constituent from Persson (2000) and the properties at wet conditions are estimated values from Carlsson (1995). Due to the viscoelastic nature of wood, the softening temperature is shifted about 8°C per decade of loading frequency. Therefore, the elastic properties measured at 95°C and probably at about 1 Hz, are also valid at

Table 2. Microfibril angle (MFA) and thickness of each fibre cell wall layer for earlywood (ew) and latewood (lw). Relative composition by mass of cellulose, hemicelluloses and lignin and its densities (ρ), from Fengel and Stoll (1973) and Bergander and Salmén (2002)

	MFA (^{0})	Thickness (μm)		Relative composition (%)		
Layer		ew	lw	Cellulose	Hemi-celluloses	Lignin
ML/2	-	0.15	0.15	0	44	56
P*	-	0.1	0.1	15	33	52
S_{1+}	+70	0.1	0.2	28	31	41
S_{1-}	-70	0.1	0.2	28	31	41
S_2	α	1.7	3.7	50	31	19
S_3	-70	0.09	0.14	48	36	16
ρ (kg/m^3)				1550	1500	1300

*not ordered

Table 3. Elastic properties of the cell wall components with respect to their principle axes, longitudinal (l) and transverse (t) at different moisture contents (MC) and temperatures, from Persson (2000) and Carlsson (1995)

	12% MC 20°C	wet 20°C	wet 95°C
Lignin			
E_l, MPa	2000	2000	60
E_t, MPa	2000	2000	60
G_{lt}, MPa	750	750	22.5
ν_{tl}	0.33	0.33	0.33
ν_{tt}	0.33	0.33	0.33
Hemicelluloses			
E_l, MPa	7000	20	10
E_t, MPa	3500	10	5
G_{lt}, MPa	1750	5	2.5
ν_{tl}	0.1	0.1	0.1
ν_{tt}	0.4	0.4	0.4
Cellulose			
E_l, MPa	134000	134000	134000
E_t, MPa	27200	27200	27200
G_{lt}, MPa	4400	4400	4400
ν_{tl}	0.01	0.01	0.01
ν_{tt}	0.5	0.5	0.5

conditions prevailing at the entrance of the gap between the refiner plates (130°C and 10^4 Hz), Irvine (1985).

The specific fracture energy, G_c, was chosen as 0.5 J/m^2. This value is not experimentally verified but it is in agreement with the surface free energy used by Atack et al. (1961). However, as the calculated energy densities are proportional to G_c, the results are suited at all events for comparison of the two loading cases. An attempt to verify this value experimentally will be performed in Section 5.2.3 "Determining material parameters". The output will be presented as single fibre stress-strain curves and elastic strain energy densities.

The calculated elastic constants for the whole latewood cell wall with α = 15° and with respect to the global x-y-z system are given in Table 4. Fig. 19 shows that the apparent E-modulus, E_{yapp} versus microfibril angle is in rather good agreement compared with data from Sedighi-Gilani and Navi (2007).

Table 4. Calculated elastic constants (GPa) for the whole cell wall with respect to the global x-y-z system. Latewood fibre with α = 15°.

	12%, 20°C	wet, 20°C	wet, 95°C
E_{yapp}	27	7.5	5.2
E_{xapp}	11	4.6	2.9
G_{xyapp}	3.2	0.69	0.47

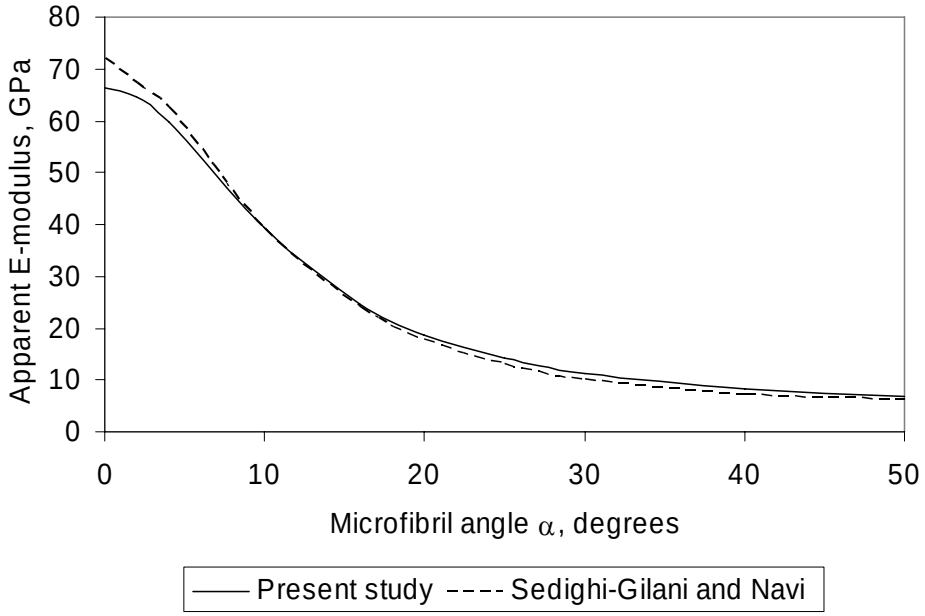

Figure 19. Apparent E-modulus in the longitudinal direction versus microfibril angle compared with data from Sedighi-Gilani and Navi (2007). Latewood fibre with α = 15°, 12% moisture content and 20°C.

Figs. 20 and 21 show respectively apparent moduli E_{yapp} and G_{xyapp} as a function of the damage state D_S. The stiffness reductions in wet condition are almost negligible although the fibre is severely damaged. This is mainly due to low stiffness of hemicelluloses in wet condition. However, the effect of the same degradation will be evident in dry condition.

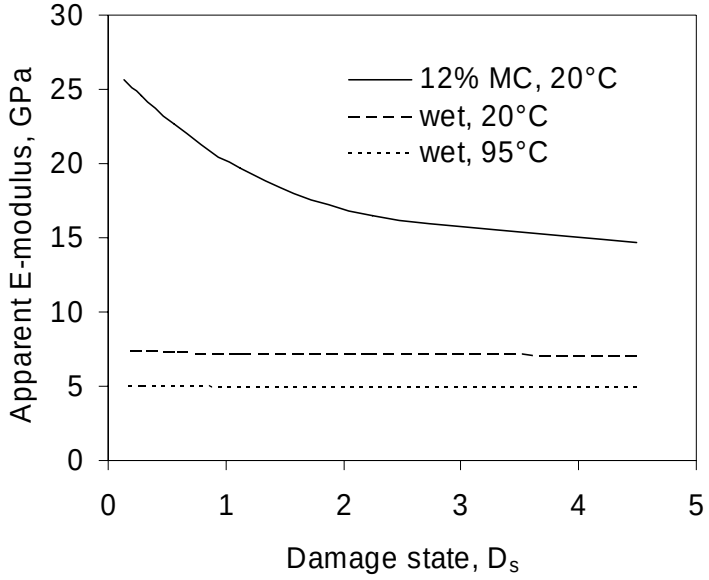

Figure 20. Degradation of apparent E-modulus in the longitudinal direction as a function of the damage state. Latewood fibre with α = 15°

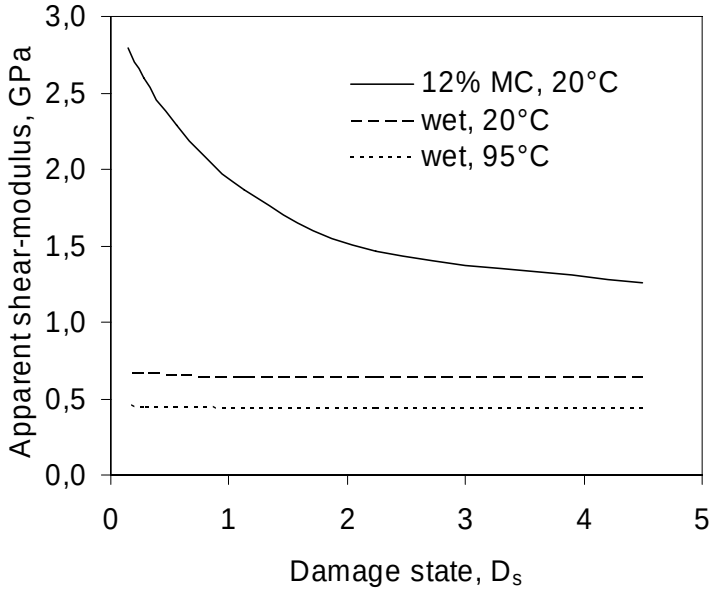

Figure 21. Degradation of apparent shear modulus as a function of the damage state. Latewood fibre with α = 15°

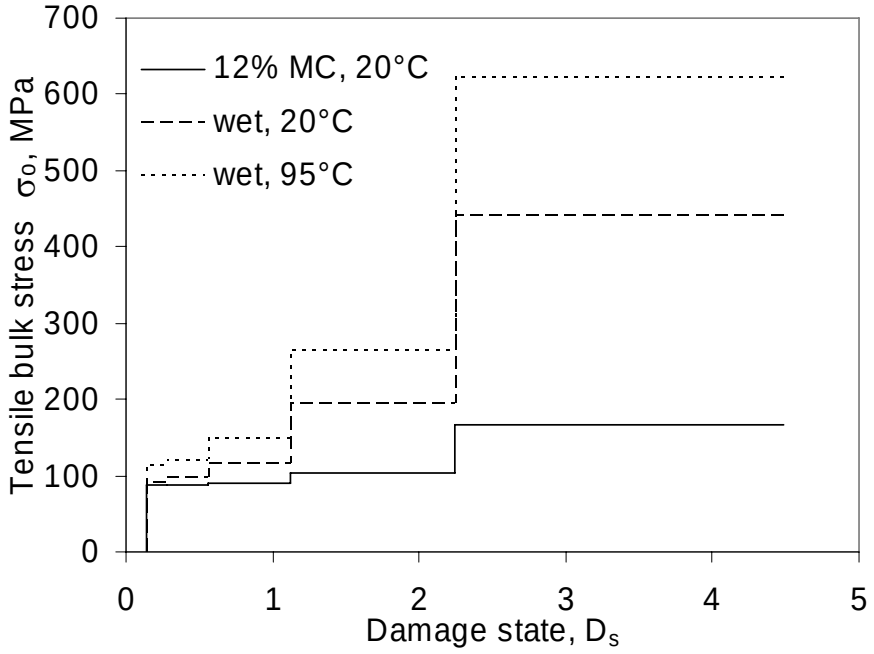

Figure 22. Tensile bulk stress as a function of the damage state
Latewood fibre with α = 15°

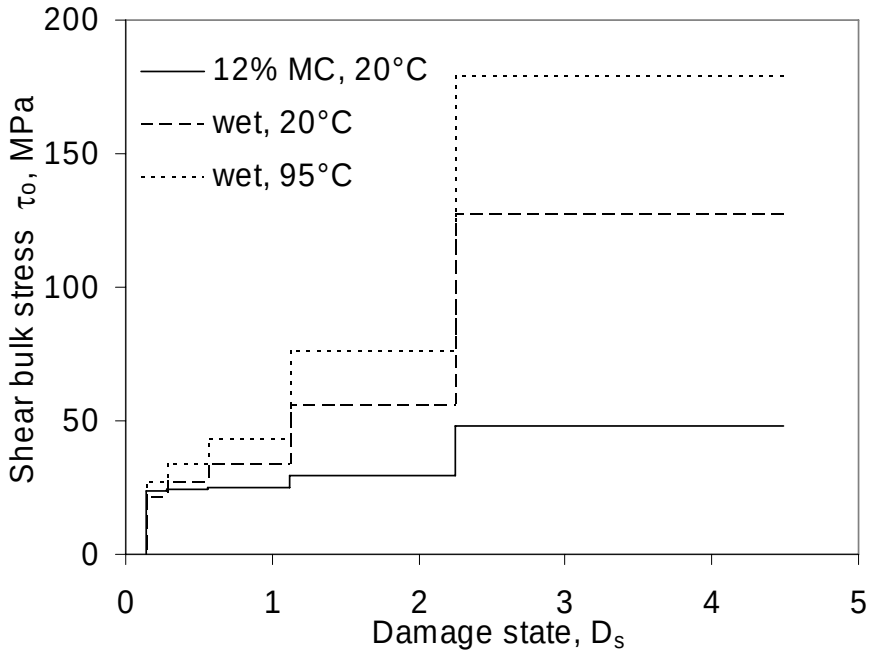

Figure 23. Shear bulk stress as a function of the damage state
Latewood fibre with α = 15°

In Figs. 22 and 23 are shown respectively the tensile bulk stress σ_0 and shear bulk stress τ_0 necessary to achieve certain damage. All fibres are loaded from D_{S0} = 0.14 to $D_{S0}\,2^4$ = 4.48, i.e. to four crack distance divisions. A tensile stress of 270 MPa or a shear stress of 76 MPa is needed to introduce a damage state, D_S = 2.24, when the fibre is wet at 95°C. In the following latewood and earlywood fibres will be compared by calculating the elastic strain energy density at a given crack distance $2d$.

The elastic strain energy per cell wall volume W_t, in a fibre subjected to uniaxial tension and at a certain stage j, can be calculated by

$$W_t = \sigma_{0,j}\varepsilon_{0,j}/2 = \sigma_{0,j}^2/(2E_{app,j}) \tag{4}$$

The necessary strain energy per area of crack surface w_t, in a fibre wall with thickness t, to create a crack distance division from $2d_0$ to d_0 in the inner layer with thickness t_1 is

$$w_t = t\,d_0\sigma_{0,j}^2/(2\,t_1E_{app,j}) \tag{5}$$

The elastic shear strain energy per area of crack surface w_s in a fibre wall, ACDB in Fig. 18 b, subjected to uniaxial shear can similarly be calculated by

$$w_s = t\,d_0\tau_{0,j}^2/(2\,t_1G_{app,j}) \tag{6}$$

Assuming initially unloaded conditions means that the energy can be termed as consumed.

Figs. 24 a-d show the elastic strain energy density versus crack distance $2d$, at different microfibril angles α, at wet conditions and 95°C. At short crack distances, 4 μm for latewood and 2 μm for earlywood, the energy consumption for crack development generally increases with higher microfibril angles α.

Contrary to ambient conditions [cf. Fig 4, Paper IV], the energy density at conditions prevailing at the entrance of the refining zone is mainly lower for earlywood compared to latewood fibres. This result is in agreement with Reme, Johnsen and Helle (1999), and Pöhler and Heikkurinen (2003) who showed that thin-walled earlywood fibres are more prone to fibre wall splitting than thick-walled latewood fibres.

Figs. 24 a-d also show that the energy density is lower for loading in shear compared to tension for both earlywood and latewood fibres at microfibril angles α=5 and 15°, actually for all $\alpha\leq$17° for latewood and $\alpha\leq$18° for earlywood according to calculations not presented here.

a)

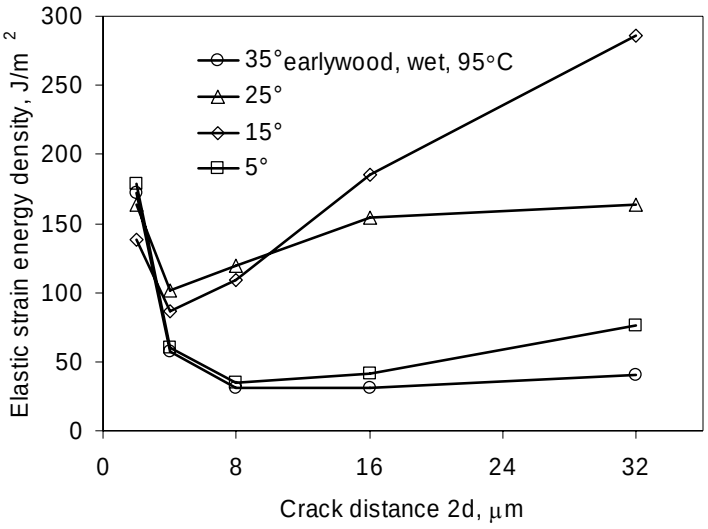
Elastic strain energy density, J/m 2
300
250
200
150
100
50
0
35°earlywood, wet, 95°C
25°
15°
5°
0
8
16
24
32
Crack distance 2d, μm

b)

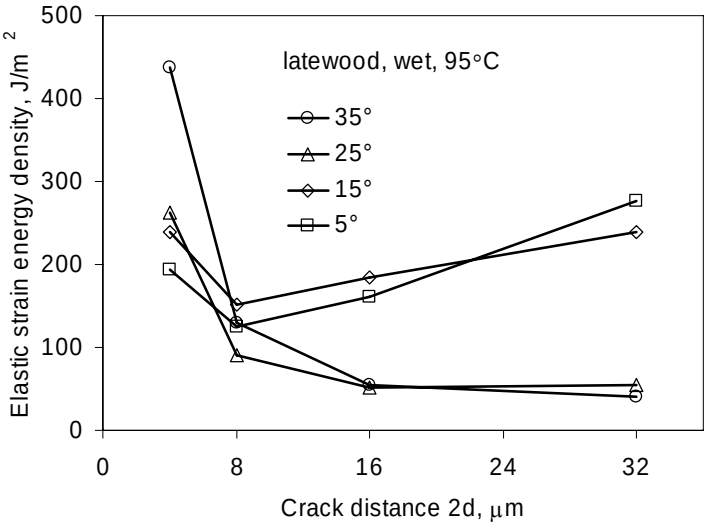
Elastic strain energy density, J/m 2
500
400
300
200
100
0
latewood, wet, 95°C
35°
25°
15°
5°
0
8
16
24
32
Crack distance 2d, μm

c)

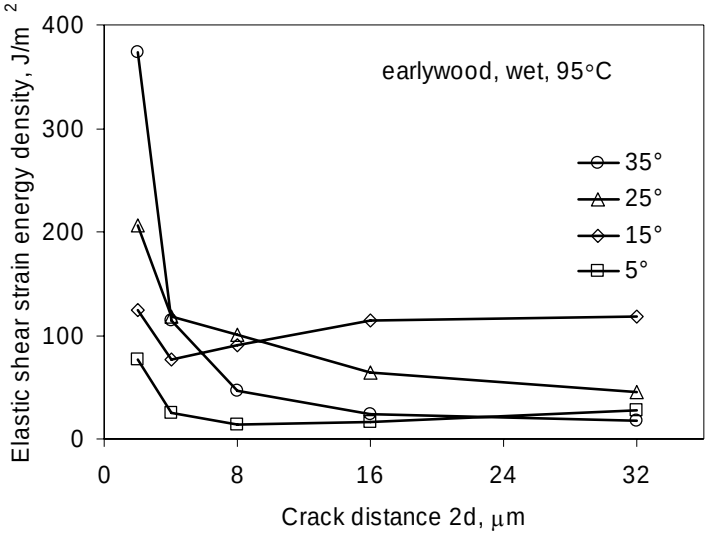

d)

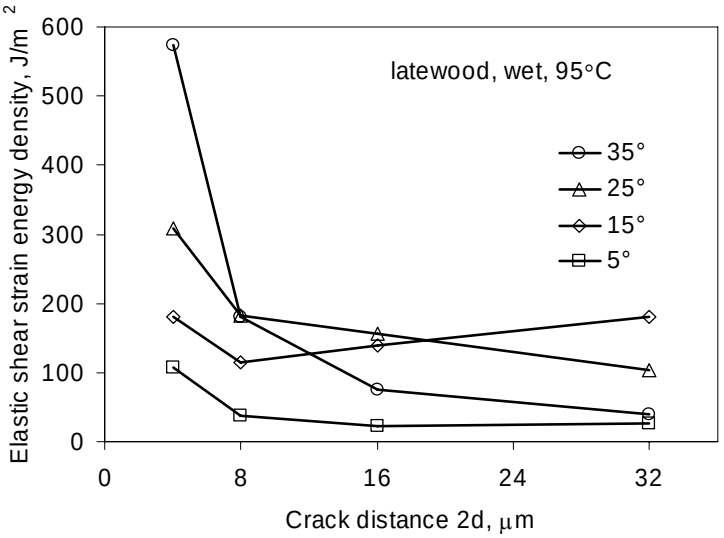

Figure 24. Elastic strain energy density versus crack distance 2d, at different microfibril angles, wet condition and temperature 95°C. a) uniaxial tension, earlywood; b) uniaxial tension, latewood; c) uniaxial shear, earlywood; d) uniaxial shear, latewood

The energy density acquired to achieve one crack distance division, is also dependent on the damage state in the fibre wall. A latewood fibre with α=5° requires about 37 J/m^2, by loading in uniaxial shear, to achieve crack distance 8 μm and 107 J/m^2 to achieve crack distance 4 μm, the corresponding values for an earlywood fibre are 14 and 25 J/m^2, Figs. 24 c-d.

5.2.1 The stress-strain curve

The development of strain ε_0 for a given stress σ_0 for wood fibres loaded in uniaxial tension, at 12% MC and temperature 20°C, is shown in Fig. 25. All fibres are loaded from the initial damage state $D_{S0}\ 2^0 = 0.14$ to $D_{S0}\ 2^4 = 4.48$, i.e. to four crack distance divisions which are indicated with symbols. For clarity reasons the divisions are not indicated for all curves. The microfibril angle α, was varied between 5 to 45°. A stiffness reduction with increased strain can be seen.

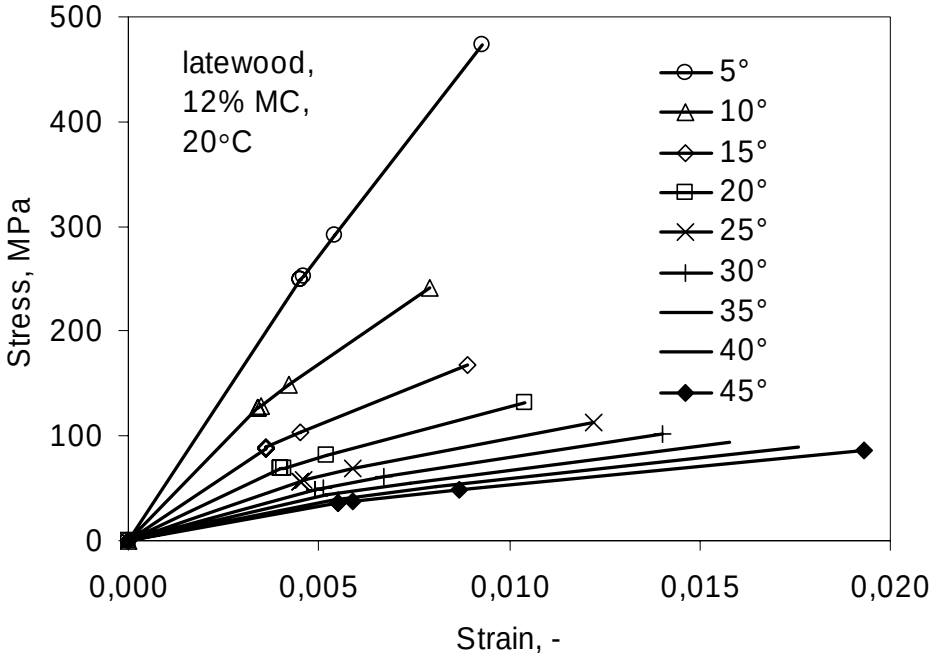

Figure 25. Analytically derived single fibre stress-strain curves at 12% MC and temperature 20°C. The microfibril angle α was varied between 5 to 45°. The crack distance divisions are indicated. For clarity reasons the divisions are not indicated for all curves.

5.2.2 Determining material parameters

It should now be possible to fit the analytically derived curves to experimental data. In the present study the data by Sedighi-Gilani and Navi (2007) will be used. They performed stress-strain tests on mechanically isolated fibres. Most fibres had microfibril angles above 20°, based on measurements at two to four points along the fibres, and showed the behaviour of an elasto-plastic material with positive hardening. One curve with α=19°, from which four data points are indicated in Fig. 26, showed a behaviour that could be explained solely by a deterioration of the fibres, i.e. the analytical model.

The parameters in the model that are fitted with respect to the experimental data are the specific fracture energy, G_C and the initial damage state, D_{S0} as described in Paper IV.

The results from the optimisation are presented in Fig. 26 with G_C =31 J/m^2 and D_{S0}=0.14. The thickness of the fibre wall layers were restricted to be among those given in Table 2, either corresponding to an earlywood or a latewood fibre.

The best fit to experimental data of the curve in Fig. 26 was found to be thicknesses related to a latewood fibre. However, the thickness of ML/2 was set to zero because most of the ML is destroyed in the mechanical isolation method as shown and described by Burgert et al. (2002) and Sedighi-Gilani and Navi (2007). The elastic properties of the cell wall components were chosen according to Table 3.

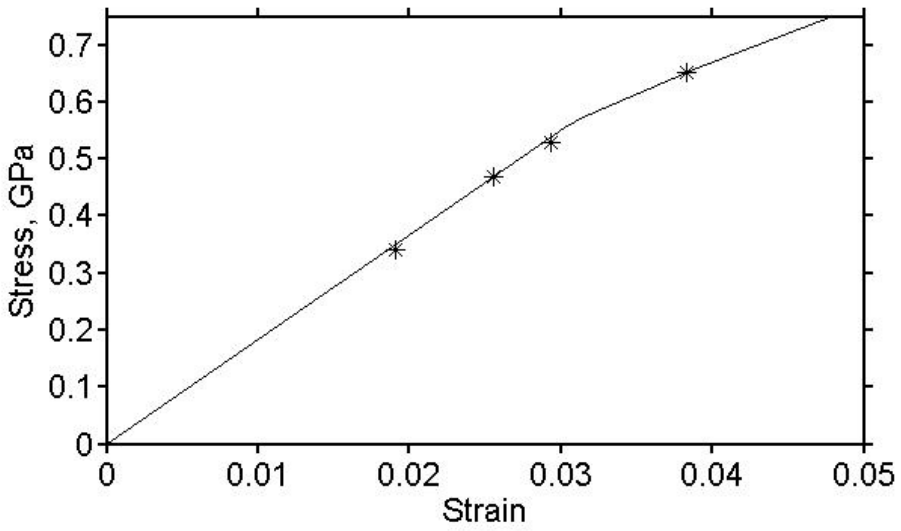

Figure 26. Analytically derived single fibre stress-strain curve at 12% MC, temperature 20°C and microfibril angle α=19° compared with experimental data from Sedighi-Gilani and Navi (2007).

5.3 Discussion

The energy consumption to achieve crack distance between 8 to 32 μm in the fibre wall by shear loading is varying between 14-180 J/m^2, Fig. 24 c-d. The model therefore predicts, with G_C=0.5 J/m^2, an energy efficiency to create cracks in the fibre wall to range from 0.5/180=0.28% to 0.5/14=3.6%. These efficiencies are in agreement with results of May (1973), who's calculations gave a theoretical energy efficiency of 1%.

However, Sundholm (1993) suggested that the refining efficiency is in the range of 40-60%. This author also pointed out that a large proportion of mechanical action is necessary to develop fibre properties. These statements were based on trials at extremely low stone speed in a pilot wood grinder.

The specific fracture energy G_C determined to 31 J/m^2, was based on only one stress-strain curve and is therefore uncertain. This is the reason why the value used by Atack et al. (1961) was taken in the energy consumption calculations.

5.4 Conclusions

Based on the assumptions in the model, the energy consumption for crack development is found to be dependent on the microfibril angle in the middle secondary wall, the loading case, the thicknesses of the cell wall layers, the damage state and conditions such as MC and temperature.

The energy consumption for crack development at conditions prevailing at the entrance of the gap between the refiner plates:

- increases, at short crack distances, with higher microfibril angles α
- is mainly lower for earlywood compared to latewood fibres
- is lower for loading in shear compared to tension for both earlywood and latewood fibres at microfibril angles α lower than 17°.

It is possible to simulate stress-strain curves for single fibres by the model together with an iterative procedure. The stiffness is reduced with increased strain.

The usefulness of the analytical model has been demonstrated by fitting input parameters to experimental data by Sedighi-Gilani and Navi (2007).

6 POWER DISTRIBUTION IN A SINGLE DISC REFINER (PAPER V)

In a typical TMP mill, approximately 80-90 percent of the applied electric power is used in the primary, secondary, and reject refiners. The applied electric energy is transformed into heat, when the material is being developed into fibres in the narrow gap between one rotating disc (rotor) and one stationary disc (stator). Both discs are equipped with patterned segments [cf. Section 1, Fig. 2], which will have different configurations depending on the desired final product.

Even though many relationships relating specific energy consumption and pulp quality have been developed over the years more has to be learned about how the supplied power is distributed within the refining zone. A tangential force sensor was, therefore, developed by which it is possible to determine the power intensity distribution within the refiner. With this knowledge, it was possible to improve, at least to some extent, theoretical and numerical models for the refining process.

6.2 Theory

In Fig. 27 a schematic view of a refiner disc together with a sensor bar is shown. Two strain gauges (represented by G) are shown on a slotted bar (S) and on a continuous bar (C).

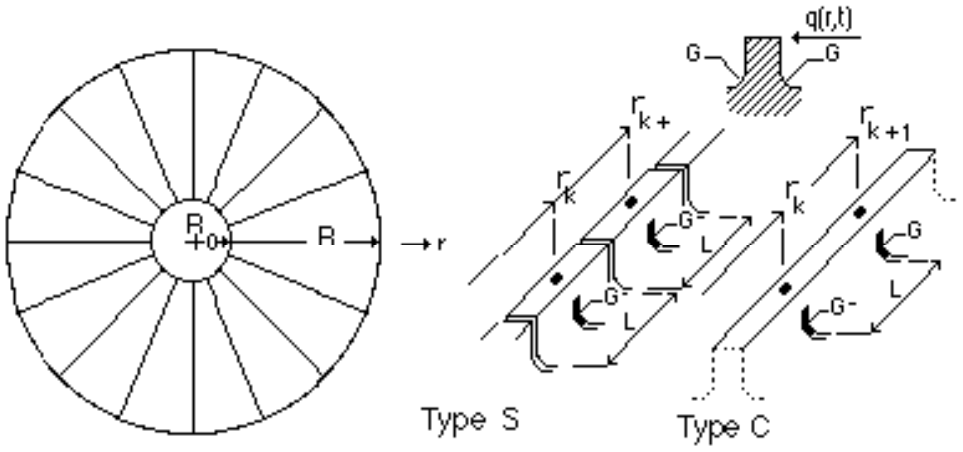

Figure 27. Schematic of a sensor bar

Two approaches are considered theoretically. In the first approach, the sensor bar is slotted so that an isolated part or subsegment with length L and its midpoint at a radial distance r_k is obtained (S in Fig. 27). In the second approach, the sensor bar is assumed to be continuous (C in Fig. 27). The theory for the continuous bar sensor is given in Paper V.

6.1.1 Slotted Sensor (S)

Assume that the tangential force intensity *q(r,t)*, see Fig. 27, is approximately constant over the subsegment length L and equal to $q(r_k,t)$ for a particular subsegment. If the subsegment is assumed to be linear elastic, the measured strain ε will depend on the total tangential force *qL* through:

$$\varepsilon(r_k,t) = k(r_k)q(r_k,t)L \tag{7}$$

where $k(r_k)$ is the influence coefficient for a subsegment having its midpoint at the radial distance r_k. Assuming that a stationary process is studied, any time average of ε and q taken over a sufficiently long time will be a function of r only. Denoting such a time average with an asterisk, one will have from Eq. (7):

$$\varepsilon^*(r_k) = k(r_k)q^*(r_k)L \tag{8}$$

and hence:

$$q^*(r_k) = \varepsilon^*(r_k)/(k(r_k)L) \tag{9}$$

The power transferred up to a point r_n; $P(r_n)$ can be approximated by:

$$P(r_n) = \omega L\sum_{k=1}^{n} q^*(r_k)r_k N(r_k) \tag{10}$$

where N is the number of bars and ω is the angular velocity. Substituting q^* from Eq. (9) in Eq. (10) will give:

$$P(r_n) = \omega\sum_{k=1}^{n} \varepsilon^*(r_k)r_k N(r_k)/k(r_k) \tag{11}$$

6.2 Test setup

The slotted (S) tangential force sensor (shown not to scale in Fig. 28) was evaluated in both primary and secondary stage refining. The trials were carried out in a Sunds Defibrator OVP-20 pilot plant, consisting of a 500 mm (20") diameter single disc refiner operating at 1500 rpm.

The inner radius of the fixed disc (R_0 in Fig. 27) was 100 mm. In order to protect the strain gauges on the sensor from the harsh environment within the refining zone, a special fastening support was developed. The sensor was installed as a separate entity from the backside of the refiner segment and soft silicone was used to protect the sensitive instrumentation, Fig. 28. To increase the sensitivity to tangential loading, the slotted sensor was manufactured in aluminium.

6.3 Typical results and discussion

By applying Eq. (11) to the measured strains of all sensor subsegments, the accumulated power *P(r)* is readily computed. The total power *P(r)* transferred up to a radius *r* is given by:

$$P(r) = \int p(r)dA = \int \tau(r) 2\pi r \frac{n}{60} dA = \int_{R_0}^{r} \tau(r)\pi^2 r^2 \frac{n}{15} dr \qquad (12)$$

where *p(r)* is power per unit area *n* is revolutions per minute and *τ(r)* is tangential force per area.

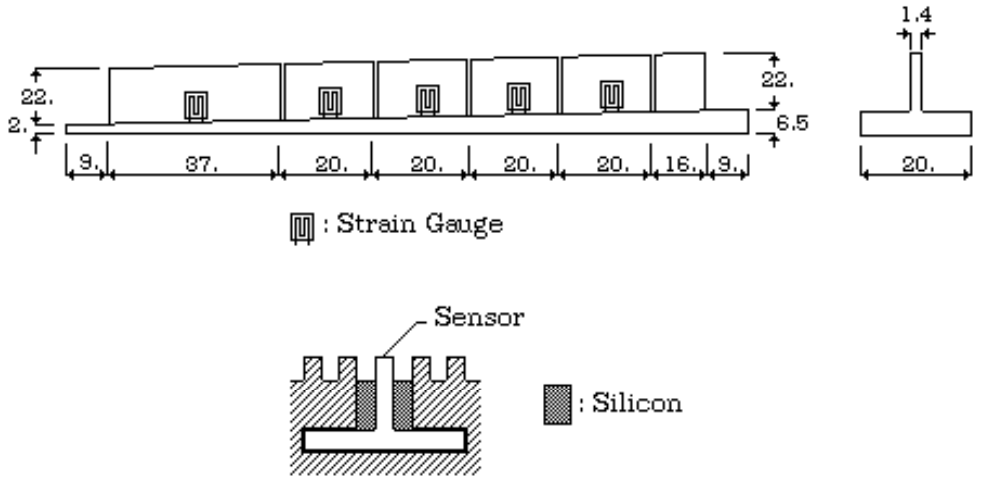

Figure 28. Slotted Sensor. Dimensions in mm

Fig. 29 shows the accumulated power normalized with respect to the total power (40 kW), P_n, together with the disc area normalized with respect to the total area of the fixed disc, A_n, as a function of the radial position, for a second-stage TMP refiner. Note that points A and B in Fig. 29 for P_n are not a result from the measurements but are given by the fact that the power equals zero on the inner radius R_0 of the fixed disc and equals the total power on the outer radius R.

A function $f = B(r^a - R_0^a)$, where $r \geq R_0$ and B is a constant, can be fitted to the normalized accumulated power P_n with a =4.74 which, according to Eq. 12, implies that the power per unit area, $p(r)$ is a function of the radius raised to the power of 2.74 and that the tangential force per area, $\tau(r)$ is a function of the radius raised to the power of 1.74. Fig. 30 shows $\tau(r)$ consistent with P_n in Fig. 29 i.e. $\tau(r)=kr^{1.74}$, k=136, as a function of the radial position.

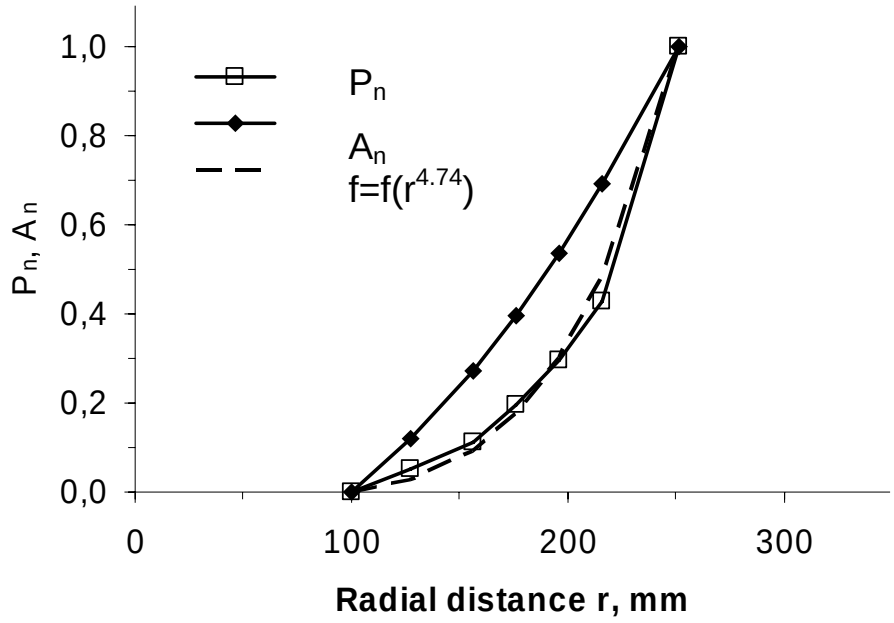

Figure 29. Normalized power and area versus radial distance

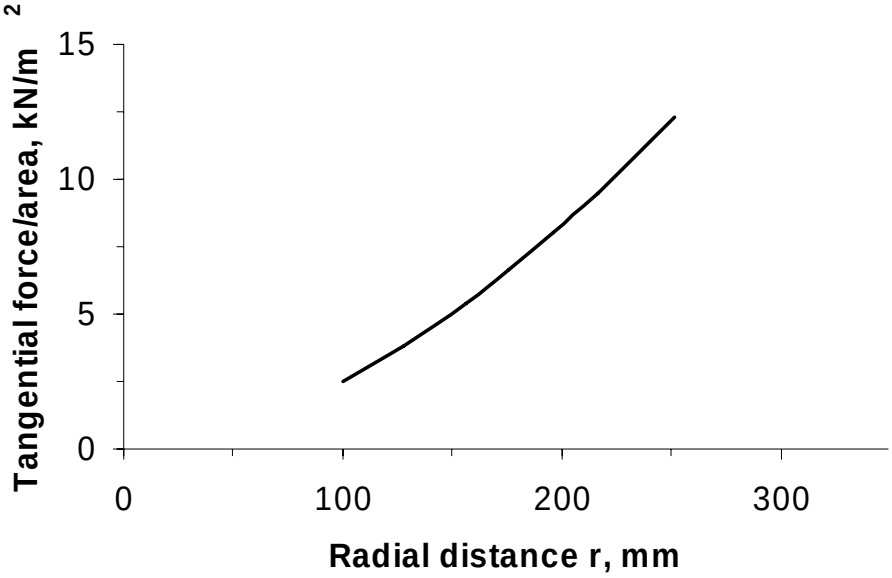

Figure 30. Tangential force per area versus radial distance

Also Backlund, Höglund and Gradin (2003) found that the tangential force increased along the radius. They performed trials on a first stage single disc refiner (SD 65) and a one stage conical disc refiner (RGP 82 CD).

6.4 Conclusions

Investigations have been carried out with different operating conditions in a 500mm (20") laboratory single-disc refiner operating under pressurized conditions at 1500 rpm.

It was found that the developed sensor is an effective way of measuring the power distribution within the refining zone. The collected data show that the tangential force per unit area and consequently also the power per unit area on a bar increases with the radial position, for a second-stage TMP refiner.

7 GENERAL CONCLUSIONS AND SUGGESTIONS FOR FUTURE WORK

In order to achieve substantial changes in the wood structure during feeding of chips into preheaters and refiners, it is crucial that:

- the wood is compressed in the longitudinal direction;
- the compression is carried out at temperatures well below 120°C; and
- the longitudinal compression should be carried out to about 20%, corresponding to a specific energy input of 3 kWh/ton.

The effect of impact velocity on the fracture of wood has been studied. Fracture of wood takes place in the breaker bar zone of the refiner plate where most of the wood is separated into single fibres.

- The experiments show that an increase in impact velocity from 2.7 to 4.8 m/s increases the impact strength by about 50%.
- The increase in impact strength with increased velocity is explained by a more shear-dominated fracture together with an increase in kinetic energy.

Screws would therefore be preferred before refiners for the initial defibration.

A micromechanical model for the deterioration of a wood fibre has been presented. The model is based on a number of simplifying assumptions. However, the model should be useful to make at least qualitative predictions.

Based on the assumptions in the model, the energy consumption for crack development is found to be dependent on the microfibril angle in the middle secondary wall, the loading case, the thicknesses of the cell wall layers, the damage state and conditions such as moisture content and temperature.

The energy consumption (EC) for crack development at conditions prevailing at the entrance of the gap between the refiner plates:

- EC increases, at short crack distances, with higher microfibril angles α
- EC is mainly lower for earlywood compared to latewood fibres
- EC is lower for loading in shear compared to tension for both earlywood and latewood fibres at microfibril angles α lower than 17°.

It would therefore be preferred to refine earlywood and latewood fibres separately.

The usefulness of the model has been demonstrated by fitting input parameters as specific fracture energy and initial damage state to experimental data.

In the future, it would be interesting to measure stress-strain or shear stress-shear strain curves on single fibres or fibre bundles at refining conditions in a laboratory setup. Such experiments would hopefully give further information of the mechanisms of the deterioration of the fibre wall.

Investigations have been carried out with different operating conditions in a 500mm (20") laboratory single-disc refiner operating under pressurized conditions at 1500 rpm.

It was found that the developed sensor is an effective way of measuring the power distribution within the refining zone. The collected data show that the tangential force per unit area and consequently also the power per unit area on a bar increases with the radial position, for a second-stage TMP refiner.

It is believed that the results from measurements and calculations suggested it this thesis, coupled with measurements on full size equipment, will be a useful tool in the struggle for lowering the energy consumption of the thermomechanical pulping process.

ACKNOWLEDGEMENTS

I would like to thank my supervisors at Mid Sweden University; Professor Per Engstrand for encouraging discussions, Professor Per A. Gradin for his continuous support throughout the PhD project and Professor Hans Höglund for many valuable comments on the thesis. I would also like to thank Staffan Nyström for designing most parts of the experimental setups and Max Lundström for his assistance in the laboratory.

The financial support of the National Board for Industrial and Technical Development, the Foundation for Knowledge and Competence Development, and Fibre Science and Communication Network, FSCN at Mid Sweden University is gratefully acknowledged as well as the technical support of SCA and Metso Paper (formerly Sunds Defibrator).

REFERENCES

Ansell, M. P. (1982)
Acoustic emission from softwoods in tension
Wood Sci. Tech. 16(1982):1, 35-58

Atack, D. (1972)
On the characterization of pressurized refiner mechanical pulps
Svensk Papperstid. 75(1984):3, 89–94

Atack, D., May, W. D., Morris E. L. and Sproule, R. N. (1961)
The energy of tensile and cleavage fracture of black spruce
Tappi J. 44(1961):8, 555-567

Atack, D. (1980)
Towards a theory of refiner mechanical pulping. APPITA 34(1980):3, 223-227

Atack, D. (1981)
Fundamental differences in energy requirement between the mechanical pulping processes
Proc. Int. Mech. Pulping Conf., Oslo, Norway 1981, Session VI, no. 5, pp. 1–15.

Atack, D., Stationwala, M.I. and Karnis, A. (1984)
What happens in refining? Pulp Paper Can. 85(1984):12, T303 - T308

Atalla, R. H. and Wahren, D. (1980)
On the energy requirement in refining. Tappi J. 63(1980):6, 121-122

Backlund, H-O., Höglund, H. and Gradin, P. (2003)
Proc. Int. Mech. Pulping Conf., Quebec City, Canada 2003, pp. 379-386

Barrett, J. D. and Schniewind, A. P. (1973)
Three-dimensional finite-element models of cylindrical wood fibers
Wood Fiber 5(1973):3, 215-225

Becker, H., Höglund, H. and Tistad, G. (1977)
Frequency and temperature in chip refining. Paperi ja Puu, 59(1977):3, 123-130

Bergander, A. and Salmén, L. (2002)
Cell wall properties and their effects on the mechanical properties of fibers
J. Mater. Sci. 37(2002):1, 151-156

Björkqvist, T., Lautala, P., Saharinen, E., Paulapuro, H., Koskenhely, K. and Lonnberg, B. (1997)
Behavior of spruce sapwood in mechanical loading
Proc. Int. Mech. Pulping Conf., Stockholm, Sweden 1997, pp. 199-205

Burgert, I., Keckes, J., Frühmann, K., Fratzl, P. and Tschegget, S. E. (2002)
A comparison of two techniques for wood fiber isolation evaluation by tensile tests on single fibers with different microfibril angle. Plant Biology 4 (2002):1, 9-12.

Campbell, W.B., (1934)
Groundwood studies. Theoretical efficiency. Pulp Paper Can. 35(1934):4, 218-219

Carlsson, P. (1995)
Analys av deformationer och spänningar i barrvedens cellväggar
M.Sc. Thesis, STFI and KTH 1995, in Swedish.

Carter, J.A., Fagans, K.P., Perry, F.G., Sparrow, D.B. and Little, A.D. (1975)
Mechanical pulps in newsprint: An economic key to the treasure map. Proc. Int. Mech. Pulping Conf., San Francisco, California, USA, 1975, part II, pp. 65-89

Côté, W.A., Jr. (1967)
Wood Ultrastructure: an atlas of micrographs. University of Washington Press, Seattle, USA.

DeBaise, G. R., Porter, A. W. and Pentoney, R. E. (1966)
Morphology and mechanics of wood fracture. Mater. Res. Standards 6(1966):10, 493-499

Dinwoodie, J. M. (1968)
Failure in timber. Part 1. Microscopic changes in cell wall structure associated with compression failure. J. Inst. Wood Sci. 21(1968), 37-53

Dinwoodie, J. M. (1974)
Failure in timber. Part 2. The angle of shear though the cell wall during longitudinal compression stressing. Wood Sci. Tech. 8(1974), 56-67

Dumail, J.F. and Salmén, L. (1997)
Compression behaviour of saturated wood perpendicular to grain under large deformations - Comparison between water-saturated and ethylene glycol-saturated wood
Holzforschung 51(1997):4, 296-302

Eskelinen, E., Hu, S. H. and Marton, R. (1982)
Wood mechanics and mechanical pulping, APPITA 36(1982):1, 32-38

Fahlén, J. (2005)
The cell wall ultrastructure of wood fibres - Effects of the chemical pulp fibre line.
Ph.D. Thesis, Royal University of Technology, KTH, Stockholm, Sweden
Trita-FPT-Report, ISSN 1652-2443 ; 2005:2, 70 p

Falk, B., Jackson, M. and Danielsson, O. (1987)
The use of single and double disc refiner configurations for the production of TMP for filled super calendered and light weight coated grades. Proc. Int. Mech. Pulping Conf., Vancouver, British Columbia, Canada, 1987, pp. 137-143

Fengel, D. and Stoll, M. (1973)
Variation in cell cross-sectional area, cell-wall thickness and wall layers of spruce tracheids within an annual ring. Holzforschung 27(1973):1,1–7

Franzén, R. (1986)
General and selective upgrading of mechanical pulps.
Nordic Pulp Paper Res. J. 1(1986):3, 4-13.

Frazier, W. C. and Williams, G. J. (1982)
Reduction of specific energy in mechanical pulping by axial precompression of wood, Pulp Paper Mag. Can. 83(1982):6, T162-T167

Gamstedt, K. (1995)
Fatigue mechanisms in unidirectional composites, Licentiate thesis, Luleå University of Technology , Sweden (1995), ISSN 0280-8242

Gillis, P. P. and Mark, R. E. (1973)
Analysis of shrinkage, swelling, and twisting of pulp fibers
Cellulose Chem. Tech. 7(1973):2, 209-234

Goring, D. A. I. (1963)
Thermal softening of lignin, hemicelluloses, and cellulose
Pulp Paper Mag. Can. 64(1963):12, T517-T527

Hamad, W. Y. and Provan, J. W. (1995)
Microstructural cumulative material degradation and fatigue-failure micromechanisms in wood-pulp fibres, Cellulose 2(1995):3, 159-177

Hartler, N. (1963)
Some studies on the nature of the chip damage, Svensk Papperstidning 66(1963):11, 443-453

Hartler, N. (1986)
Wood quality requirements in mechanical pulping
Nordic Pulp Paper Res. J. 1(1986):1, 4-10.

Hattula, T. and Mannström, B. (1981)
Wood structure as a limiting factor in mechanical pulping
Proc. Int. Mech. Pulping Conf., Oslo, Norway 1981, Part I, pp. 1-21

Heikkurinen, A. Vaarasalo, J. and Karnis, A. (1993)
Effect of initial defiberization on the properties of refiner mechanical pulp
J. Pulp Paper Sci. 19(1993):3, J119-J124

Hoekstra, P., Veal, M. and Lee, P. (1983)
The effects of chip size on mechanical pulp properties and energy consumption
Tappi J. 66(1983):9, 119-122.

Holmberg, S. (1996)
Deformation and fracture of wood in initial defibration processes, Licentiate thesis, Lund University, Sweden 1996, Report TVSM-3019, ISSN 0281-6679, 113 p

Holmberg, S. (1998)
A numerical and experimental study of initial defibration of wood
Ph.D. Thesis, Lund University, Sweden 1998, Report TVSM-1010, ISSN 0281-6679, 203 p

Holmgren, S.-E., Svensson, B.A., Gradin, P.A. and Lundberg, B. (2008)
An encapsulated Split Hopkinson pressure bar for testing of wood at elevated strain rate, temperature, and pressure. Exp. Tech. 32(2008):5, 44-50

Härkönen, E., Huusari, E. and Ravila. P. (1999)
Residence time of fiber in a single disc refiner
Proc. Int. Mech. Pulping Conf., Houston, Texas, USA, 1999, pp. 77-86.

Härkönen, E., Kortelainen, J. and Virtanen, J. (2003)
Fiber development in TMP main line
Proc. Int. Mech. Pulping Conf., Quebec City, Canada, 2003, pp. 171-178

Härkönen E. and Tienvieri T. (1995)
The Influence of Production Rate on Refining in a Specific Refiner
Proc. Int. Mech. Pulping Conf., Ottawa, Canada, 1995, pp. 177-182

Höglund, H., Bäck, R. Falk, B. and Jackson, M. (1995)
Thermopulp - a new energy efficient mechanical pulping process
Proc. Int. Mech. Pulping Conf., Ottawa, Ontario, Canada 1995, pp. 213-225

Höglund, H., Sohlin, U. and Tistad, G. (1976)
Physical properties of wood in relation to chip refining, Tappi J. 59(1976):6, 144-147

Höglund, H. and Tistad, G. (1973)
Energy uptake by wood in the mechanical pulping process
Proc. Int. Mech. Pulping Conf., Stockholm, Sweden 1973, pp. 3:1-3:15

Irvine, G. M. (1984)
The glass transitions of lignin and hemicellulose and their measurement by differential thermal analysis. Tappi J. 67(1984):5, 118–121

Irvine, G. M. (1985)
The significance of the glass transition of lignin in thermomechanical pulping
Wood Sci. Tech. 19(1985),139–149

Irwin, G. R. (1958)
Handbook der Physik, Springer, Berlin, Germany 6(1958), pp. 551-590 (S. Flügge editor)

Jang, HF., Weigel, G, Seth, RS. and Wu, CB. (2002)
The effect of fibril angle on the transverse collapse of papermaking fibres
Paperi ja Puu 84(2002):2, 112-115

Johansson, L., Peng, F.F., Simonson, R. and Granfeldt, T (1999)
The effects of chip pretreatment on CTMP pulp properties. Paperi ja Puu 81(1999):8, 559-564

Karnis, A. (1994)
The mechanism of fibre development in mechanical pulping
J. Pulp Paper Sci. 20(1994):10, J280-J288

Kawamoto, S. and Williams, R.S. (2002)
Acoustic emission and acousto-ultrasonic techniques for wood and wood-based composites—A review. Gen. Tech. Rep. FPL-GTR-134. Madison, WI: U.S. Department of Agriculture, Forest Service, Forest Products Laboratory. 16 p.

Kelley, S.S., Rials, T.G. and Glasser, W.G. (1987)
Relaxation behavior of the amorphous components of wood.
J. Mater. Sci. 22(1987), 617-624.

Kivimaa, E. and Murto, J. (1949)
Investigations on factors affecting the chipping of pulp wood
VTT Publication : 9 Helsinki, Finland, 1949, 25 p.

Koran, Z. (1979)
Tensile properties of spruce under different conditions. Wood Fiber 11(1979):1, 38-49

Kure, K.-A. (1997)
The alteration of the wood fibres in refining
Proc. Int. Mech. Pulping Conf., Stockholm, Sweden, 1997, pp. 137-150

Kure, K.-A., Dahlqvist, G., Sabourin, M.J. and Helle, T. (1999)
Development of spruce fibre properties by a combination of a pressurized compressive pre-treatment and high intensity refining
Proc. Int. Mech. Pulping Conf., Houston, Texas, USA, 1999, pp. 427 - 433

Kärenlampi, P.P., Tynjälä, P. and Ström, P. (2003)
The effect of temperature and compression on the mechanical behavior of steam-treated wood. J. Wood Sci. 49(2003):4, 298-304

Lamb, G. (1960)
The efficiency of mechanical pulping processes, Tappi J. 43(1960):11, 939-944

Mark, R. E. (1967)
"Cell wall Mechanics of Tracheids", Yale University Press 1967

Mark, R. E. and Gillis, P. P. (1970)
New models in cell-wall mechanics. Wood Fiber 2(1970):2, 79-95

Marton, R. and Eskelinen, E. (1982)
Impact testing in the study of chip refining. Tappi J. 65(1982):12, 85-89

Marton, R. Tsujimoto, N. and Eskelinen, E. (1981)
Energy consumption in thermomechanical pulping, Tappi J. 64(1981):8, 71-74

May, W. D. (1973)
A Theory of chip refining - The origin of fiber length
Pulp Paper Mag. Can. 74(1973):1, 70-78

McLauchlan, T.A. and Lapointe, J.A. (1979)
Production of chips by disc chipper, Chip Quality Monograph, Hatton, J.V. editor, Pulp and paper technology series, No 5, Joint Textbook Committee of the Paper Industry, CPPA/TAPPI, Vancouver, British Columbia, Canada, 1979

Miles, K. B. (1990)
Refining intensity and pulp quality in high-consistency refining
Paperi ja Puu 72(1990):5, 508-514

Miles, K. B. (1991)
A simplified method for calculating the residence time and refining intensity in a chip refiner Paperi ja Puu 73(1991):9, 852-857

Miles, K.B. and May, W.D. (1990)
The flow of pulp in chip refiners, J. Pulp Paper Sci., 16 (2), pp. J63-J71, 1990.

Mohlin, U. B. (1997)
Fiber Development during Mechanical Pulp Refining
J. Pulp Paper Sci. 23(1997):1, J28-J33.

Murton, KD (1995)
The effect of chip compression on TMP pulp properties
49th APPITA Annual General Conference, 3-7 Apr. 1995, Hobart, Australia, pp 337-345

Nissan, A.H. (1977)
Lectures on fiber science in paper, Pulp and paper technology series no. 4. Joint Textbook Committee of the Paper Industry, (CPPA/TAPPI), Vancouver, British Columbia, Canada, 1977, pp 27-29

Ottestam, C. and Salmén, L. (2001)
Short communication: Fracture energy of wood; relation to mechanical pulping
Nordic Pulp and Paper Research Journal 16(2001):2, 140-142

Ouellet, D., Bennington, C.P.J. Senger, J.J. Borisoff, J.F. and Martiskainen, J.M. (1996)
Measurement of Pulp Residence Time in a High Consistency Refiner
J. Pulp Pap. Sci. 22(1996):8, J301-J305

Paavilainen, L. (1993)
Conformability - flexibility and collapsibility - of sulphate pulp fibers
Paperi ja Puu 75(1993):9-10, 689-702

Peng, F. and Granfeldt, T. (1996)
Changes in the microstsructure of spruce wood chips after screw press treatment
J. Pulp Pap. Sci. 22 (1996):4, J140-J145.

Persson, K. (2000)
Micromechanical modelling of wood and fibre properties
Ph.D. Thesis, Lund University, Sweden 2000, Report TVSM-1013, ISSN 0281-6679, 213 p

Pollock, A. A. (1981)
Acoustic emission amplitude distributions, International Advances in Non destructive Testing 7(1981), 215-239 Gordon and Breach, Science Publishers, Inc., USA 1981

Pöhler, T. and Heikkurinen, A. (2003)
Amount and character of splits in fiber wall caused by disk refining
Proc. Int. Mech. Pulping Conf., Quebec, Canada 2003, pp. 417-423

Pöyry, J. (1977)
Are energy costs the Achilles' heel of mechanical Pulp?
Paperi ja Puu 59(1977):10, 604-608

Reme, P. A., Johnsen, P. O. and Helle, T. (1999)
Changes induced in early- and latewood fibres by mechanical pulp refining
Nordic Pulp Paper Res. J. 14(1999):3, 260-266

Rundlöf, M., Höglund, H., Htun, M. and Wågberg, L. (1995)
Effect of fines quality on paper properties - new aspects
Proc. Int. Mech. Pulp. Conf., Ottawa, Canada 1995, pp. 109-118

Sabourin, M. (1998)
Evaluation of a compressive pretreatment process on TMP properties and energy requirements
31st Pulp and Paper Annual Meeting, Sao Paulo, Brazil, 19-23 Oct. 1998, pp 541-555

Sabourin, M., Aichinger, J. and Wiseman, N. (2003)
Effect of increasing wood chip defibration on thermomechanical and chemi-thermomechanical refining efficiency
Proc. Int. Mech. Pulping Conf., Quebec, Canada, 2003, pp. 163-170

Salmén, L. (1984)
Viscoelastic properties of in situ lignin under water-saturated conditions
J. Mater. Sci. 19(1984):9, 3090–3096

Salmén, L. (1986)
The Cell Wall as a Composite Structure in "Paper structure and properties", Marcel Dekker Inc., New York, USA, 1986, ISBN 0-8247-7560-0 (editor J. A. Bristow)

Salmén, L., Dumail, J.F. and Uhmeier, A. (1997)
Compression behaviour of wood in relation to mechanical pulping
Proc. Int. Mech. Pulping Conf., Stockholm, Sweden 1997, 207-211

Salmén, L. and Fellers, C. (1982)
The fundamentals of energy consumption during viscoelastic and plastic deformation of wood, Transactions of the Technical Section, CPPA 8(1982):4, TR 93-TR 99

Schniewind, A. P. (1970)
Elastic behaviour of the wood fiber in "Theory and design of wood and fiber composite materials" (editor B. A. Jayne) Syracuse University Press, New York, USA

Schniewind, A. P. and Barret, J. D. (1969)
Cell-wall model with complete shear restraint. Wood Fiber 1(1969):3, 205-214

Stone, J. E. (1955)
The rheology of cooked wood, II. Effect of temperature. Tappi J. 38(1955):8, 452-459

Stone, J. E., and Nickerson, L. F. (1961)
The pulping of mechanically treated wood. Pulp Paper Mag. Can. 62(1961):6, T317-T326

Strand, B. C. and Mokvist, A. (1989)
The application of comminution theory to describe refiner performance
J. Pulp Paper Sci. 15(1989):3, J100-J105

Sundholm, J. (1993)
Can we reduce energy consumption in mechanical pulping?
Proc. Int. Mech. Pulp. Conf., Oslo, Norway 1993, pp 133-142

Sundholm, J. (ed) (1999)
Mechanical pulping in "Vol 5 of Papermaking science and technology" 1999 Helsinki: Finnish Paper Engineers' Associaton, p 428 (editors Gullichsen, J. and Paulapuro, H.)

Sundholm, J. Heikkurinen, A. and Mannström, B. (1988)
The role of rate of rotation and impact frequency in refiner mechanical pulping
Paperi ja Puu 70(1988):5, 446-451

Svensson, B.A., Holmgren, S-E, Höglund, H., Gradin, P.A. and Lundberg, B (2007)
High Strain Rate Compression of Spruce Wood in a Saturated Steam Environment
In: Frictional studies and high strain rate testing of wood under refining conditions, Svensson, B.A., Mid Sweden University Doctoral Thesis 31, Sundsvall, Sweden, 2007, ISSN 1652-893X, ISBN 978-91-85317-64-6

Tang, R. C. (1972)
Three-dimensional analysis of elastic behaviour of wood fiber
Wood Fiber 4(1972):3, 210-219

Tang, R. C. and Hsu, N. N. (1973)
Analysis of the relationship between microstructure and elastic properties of the cell wall,
Wood Fiber 5(1973):2, 139-151

Tchepel, M., Ouellet, D., Mcdonald, D., Provan, J., Skognes, G. and Steinke, D. (2003)
The responce of the long fibre fraction to different refining intensities
Proc. Int. Mech. Pulping Conf., Quebec, Canada 2003, pp. 425-436

Thorpe, J. and McLean, D. (1983)
Simulation of the effects of compression and shear on single fibers, Int. Paper Physics Conf. Harwichport, MA 1983, TAPPI, Atlanta, GA 1983, p 51-58

Tienvieri, T., Huusari, E., Sundholm, J., Vuorio, P., Kortelainen, J. Nystedt, H. and Artamo, A. (1999)
Thermomechanical pulping, In: Mechanical Pulping, Ed: J. Sundholm, Fapet Oy, Helsinki, Finland, pp. 159–221.

Uhmeier, A. (1995)
Some Aspects on Solid and Fluid Mechanics of Wood in Relation to Mechanical Pulping, Ph.D. Thesis, Royal Institute of Technology, Div. Paper Tech, Stockholm, Sweden 1995, ISSN 1104-7003

Widehammar, S. (2004)
Stress-strain relationships for spruce wood: Influence of strain rate, moisture content and loading direction. Exp. Mech. 44(2004):1, 44-48

Östberg, G., Salmén, L. and Terlecki J. (1990)
Softening temperature of moist wood measured by differential scanning calorimetry. Holzforschung 44(1990):3, 223-225